

# Experiments and Models in Enantiorecognition by Chiral Pirkle-type Stationary Phases Containing Aromatic $\pi$ -Acid Branching Units\*\*\*

Darko Kontrec, Vladimir Vinković, Maja Šepelj, and Vitomir Šunjić\*\*\*

*Rudjer Bošković Institute, P. O. Box 180, Bijenička 54, 10002 Zagreb, Croatia*

RECEIVED MAY 28, 2003; REVISED SEPTEMBER 8, 2003; ACCEPTED SEPTEMBER 8, 2003

An overview of the projects in the authors' laboratory aimed at developing novel chiral stationary phases (CSPs) is presented. Emphasis is put on the origin of the concept of using 2,4,5,6-tetrachloro-1,3-dicyanobenzene (TCDCB) and 4-chloro-3,5-dinitrobenzoic acid (CDNB) as the branching units in the Pirkle-type (brush-type) CSPs. Preparations of nearly a hundred novel CSPs, requiring synthesis of almost three hundred new compounds as intermediates or model structures, are described. Specific recognition properties and enantioselection efficacy of individual CSPs is demonstrated for various sets of test racemates (TR). Correlation between the structure and conformational properties of chiral selectors and racemic analytes is discussed. Specific properties of some CSPs, such as enhancement of their capacity by introducing the tweezer unit in the chiral selector, and catalysis of the enantiomerization process of configurationally unstable analyte are discussed. The mechanism of enantiorecognition of some TRs by structurally related CSPs is suggested.

## Key words

chiral stationary phases  
brush type  
enantioseparation  
chiral recognition mechanism

## INTRODUCTION

Aesthetically motivated supramolecular organic and organometallic synthesis, based on symmetry, topology, and network properties, constitutes a distinct goal for topics such as crystal engineering and chiral recognition. Chiral recognition or enantiorecognition represents a bottom line process that enables separation of enantiomers by chromatography on chiral stationary phases (CSPs). Enantio-recognition, and consequently enantioselection, are based on »multipoint« interactions between CSP and at least one of the enantiomers. This means that a particular CSP fits spatially one »ideal« enantiomer from the racemate in comparison with a »non-ideal« fit of the other.

Considering only one simple, isolated molecule of the chiral selector (CS) with *e.g.* only one chiral center, Dalglisch has proposed a stereoselective binding model presented in Figure 1.<sup>1</sup>

»Ideal fit« envisaged for the enantio-related chiral selector (CS) and the selectand or test racemate (TR) in this Figure suggests that the complex between CS and TR of the opposite absolute configuration should be more stable, given the overall structural similarity of the two interacting species. As we shall see, this does not hold for a series of  $\alpha$ -amino acid derivatives ( $\alpha$ -AA derivatives) and selectors based on derivatives of D-PhGly and D-Val. Actually, the »non-ideal« fit of  $\alpha$ -AAs of the *same* configuration in selectand and selector led to stronger

\* Dedicated to Professor Nenad Trinajstić on the occasion of his 65<sup>th</sup> birthday.

\*\* Based on the lecture given at the Math/Chem/Comp Conference, Dubrovnik, June 24–29, 2002.

\*\*\* Author to whom correspondence should be addressed. (E-mail: [sunjic@rudjer.irb.hr](mailto:sunjic@rudjer.irb.hr))

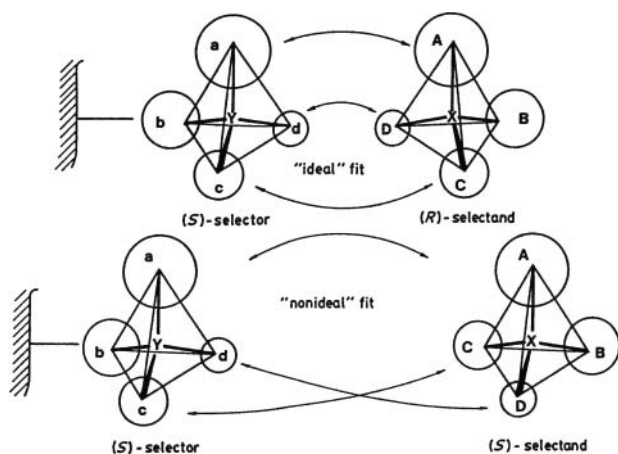


Figure 1. Stereoselective interactions, binding model of the chiral selector and racemic selectand molecule.<sup>1</sup>

binding, slowing the elution of the analyte of the same configuration.

In general, when the chiral selector is bound forming CSP, it can be clustered and organized into liquid crystal-like structures, forming a »selector surface« and internal available space, known as chiral holes or clefts, which might act synchronically or synergistically with the isolated selector-analyte chiral recognition.<sup>1</sup>

There are a few types of CSPs, which are usually divided into two groups according to the source of chirality, Figure 2.<sup>2-5</sup>

(i) brush-type or Pirkle type CSPs, based on chiral selectors covalently bound to an achiral solid support.

(ii) natural and synthetic polymers with chiral monomeric units.

This review refers to the first group of CSPs developed in our laboratory, known as Pirkle-type CSPs after Prof. W. Pirkle, the inventor and promotor of chiral HPLC methods.<sup>6,7</sup>

Various brush-type CSPs can be schematically visualized according to Figure 3.

They are characterized by covalent binding *via* spacer onto the surface of a solid support, usually silica gel, and well-defined chiral selector molecules. Their chirality is usually based on stereogenic or chiral centers. Stereoselective attractive interactions are usually based on hydrogen bonding, van der Waals (VDW), and all types of  $\pi$ - $\pi$  interactions. For some specific selectors, chiral recognition is based on inclusion phenomena, chelating by transition metals, and electrostatic (Coulombic) interactions.<sup>8-10</sup>

It is important to note that the branching unit of type **a.** is present in all commercial columns for HPLC enantio-separation developed to date. We have therefore envisaged branching unit types **b.** and **c.**, with tweezer- and dendrimer-like structures, respectively. They are promising due

to the possibility of getting higher loading capacity than type **a.** analogs, and eventual higher resolution capacity due to cooperativeness based on the multiple chiral selector unit, and their  $C_2$  and  $C_3$  symmetry.

The last decades have seen intensive research aimed at the development of new chiral stationary phases for HPLC, though the first breakthrough in this field was made by Prof. W. Pirkle and his group.<sup>6,11,12</sup> The efforts of other groups are reported in original papers that represent the milestones in this field, and are collected in recent monographs.<sup>5,8,9</sup> Contributions of Welch,<sup>13,14</sup> Gasparini,<sup>15,16</sup> Uray,<sup>17,18</sup> Lindner,<sup>19,20</sup> Allenmark,<sup>21,22</sup> Salvadori,<sup>23,24</sup> Oliveros,<sup>25,26</sup> Oi,<sup>27,28</sup> Hyun,<sup>29-31</sup> and their coworkers to this field merit particular emphasize.

Herein we report our own contribution to this field, and how the concept of tweezer-type and some related brush-type CSPs was born in our Laboratory. The results that enabled the first commercialization of HPLC columns with original CSPs developed within this project in the last 5 years are emphasized.

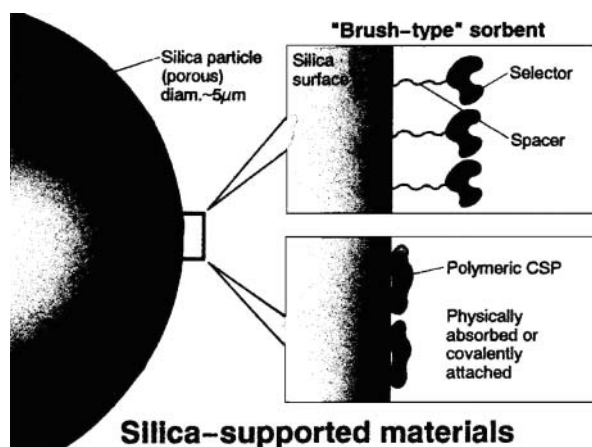


Figure 2. Schematic presentation of CSPs with silica support.<sup>2</sup>

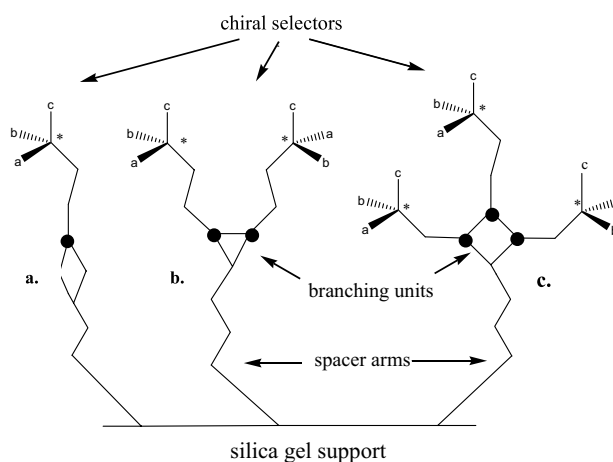
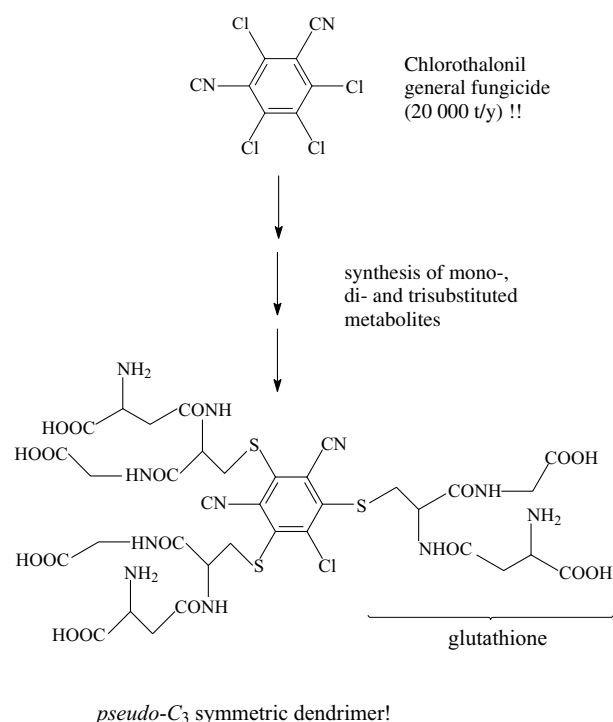


Figure 3. Schematic view of: **a.** brush-type, **b.** tweezer-type, and **c.** dendrimer-type CSPs showing the chiral selector towards the space with the mobile phase.

### The Concept and towards Its Proof

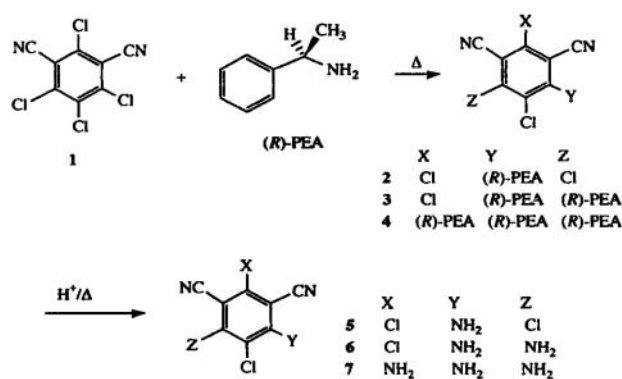
Having the above outlined concepts in mind, we started the project of the design and synthesis of novel sets of brush-type CSPs comprising, as a branching unit, a commercially available, multi-ton product, persubstituted benzene derivative, 2,4,5,6-tetrachloro-1,3-dicyanobenzene (TCDCB). Actually, the observation that the three *meta*-related chlorine atoms in TCDCB can be stepwise substituted by the thiolate anion of tripeptide glutathione, thus producing one of the metabolites of TCDCB with a dendrimeric structure, Scheme 1,<sup>32</sup> suggested preparation of these novel CSPs.



Scheme 1. Structure of dendrimeric metabolite of TCDCB with glutathione.<sup>32</sup>

According to the above scheme, di- and tri-substituted metabolites possess tweezer-type or dendrimer-type structures, and could potentially be developed into CSPs. However, none of the three amino acids in the tripeptide glutathione unit contains an aromatic ring to offer additional  $\pi$ - $\pi$  interaction with the racemic analyte, generally recognized as an important contribution to enantioselection. We have therefore prepared the first group of chiral derivatives of TCDCB, and their model achiral compounds for UV/CD and photoelectron spectroscopy (PES) studies, Scheme 2.<sup>33</sup>

The UV spectra of **5–7** are characterized by a non-monotonous change of their band maxima and intensity due to the differential degree of polarization in molecules **1** and **5–7**, depending on their overall symmetry and electronic properties of the substituents on the ring.



Scheme 2. Preparation of trisubstituted achiral and chiral amino derivatives of TCDCB.<sup>33</sup>

Combination of electron-attracting chlorine atoms and electron-donating amino groups in **5–7** produces polarization of the whole molecule, favoring various push-pull resonance forms, Figure 4.

CD spectra of optically pure (+)-phenylethylamino ((+)-PEA) derivatives **2–4** differ significantly as well, Figure 5, a phenomenon related to the observed difference in the UV spectra.

There is a strong positive couplet only in the CD of trisubstituted derivative **4** at 280 nm, revealing excitone coupling between the phenyl ring in one PEA unit and the charge-transfer system in the persubstituted ring.

To completely define the electronic structure of this branching unit in the future CSPs, we started the study using the combined PES and semiempirical PM3 method.

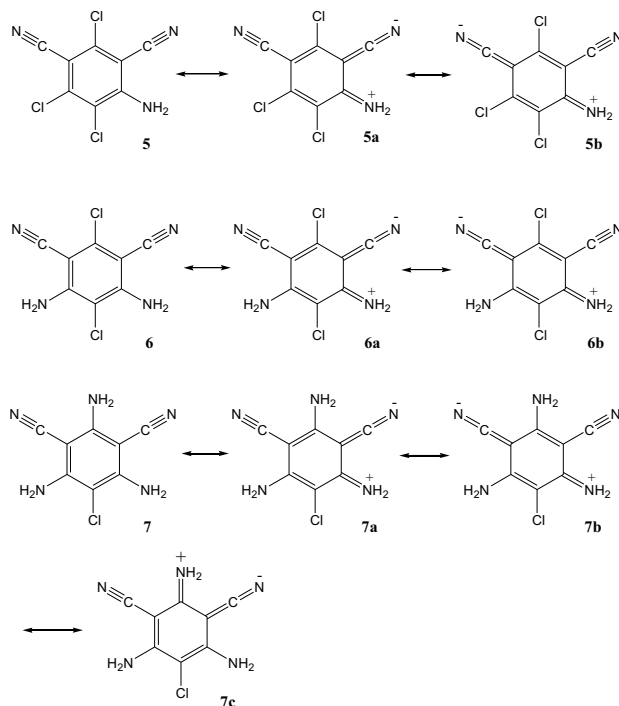
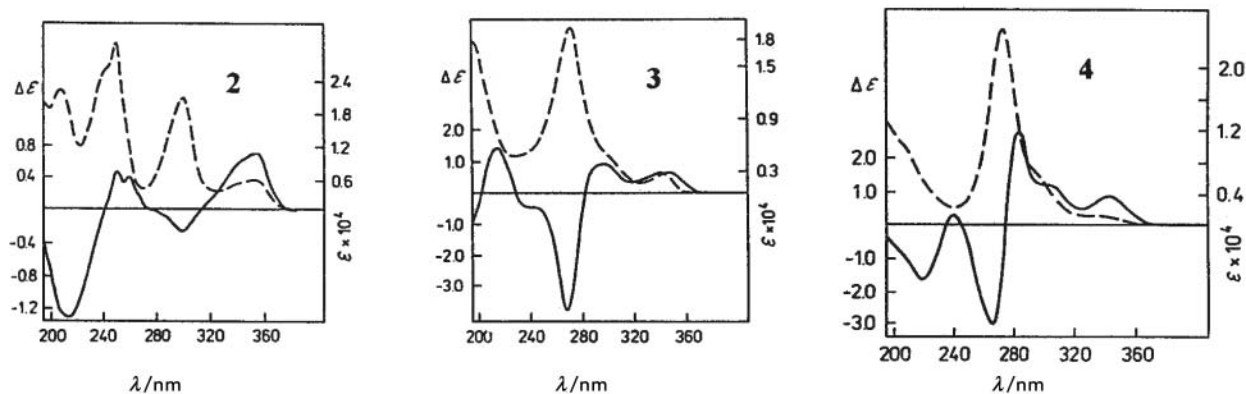
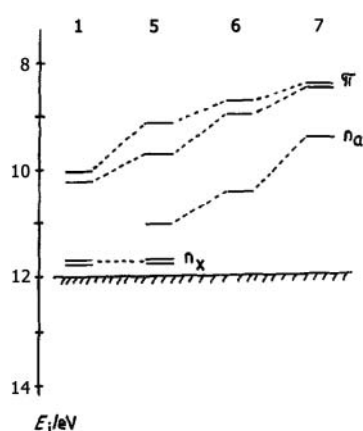


Figure 4. Resonance structures of **5–7**.<sup>33</sup>

Figure 5. CD spectra of compounds **2–4** in MeCN.Figure 6. The energy level correlation diagram for **1,5–7**, deduced from UPS (PES).<sup>34</sup>

This approach allowed an estimate of the frontier orbital energies.<sup>34</sup> The energy level diagram for compounds **1, 5–7** in Figure 6 was deduced from PES;  $n_a$  and  $n_x$  designate lone pairs from amino and chlorine substituents, respectively.

Combined UV and PES data are presented in Table I, where one can see mainly a non-additive influence of substituents on the frontier orbitals.

TABLE I. Absorption band maxima (UV / eV), 1st vertical ionization energy ( $E_1$  / eV) and estimated LUMO

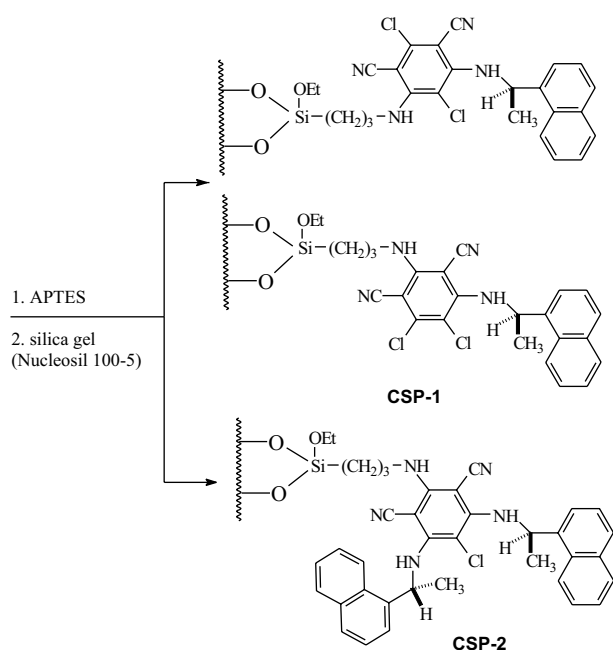
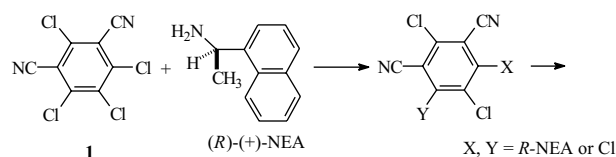
| Compound | UV ( $\epsilon \cdot 10^4$ )<br>eV $M^{-1}cm^{-1}$ | $E_1$ / eV |       |
|----------|--|------------|-------|
|          |  | -HOMO      | LUMO  |
| <b>1</b> | 5.24 (2.22)  | 10.03      | -4.64 |
| <b>5</b> | 5.11 (2.98)  | 9.17       | -3.89 |
| <b>6</b> | 4.93 (3.80)  | 8.77       | -3.70 |
| <b>7</b> | 4.89 (3.05)  | 8.43       | -3.54 |

In conclusion, all amino derivatives of TCDCB possess relatively high polarity and  $\pi$ -basicity. For their interactions in CSPs, their polarity is more important than  $\pi$ -electron density.

Summing up of the Hammett  $\sigma_m$ -values for compounds **1, 5–7** indicates strong  $\pi$ -acidity of TCDCB (**1**), but low to medium  $\pi$ -basicity of amino derivatives **5–7**.

#### CSPs Containing Persubstituted Benzene (TCDCB) as the Branching Unit

With all the above data at hand, we completed preparation of the first CSPs according to Scheme 3.<sup>35</sup>



APTES =  $\gamma$ -aminopropyl-triethoxysilane

Scheme 3. Preparation of **CSP-1** and **CSP-2**.<sup>35</sup>

On introduction of optically pure (+)-naphthylethylamine ((+)-NEA) as a stronger  $\pi$ -donor than (+)-PEA, and due to the presence of three aminoalkyl groups in the persubstituted aromatic ring, strong  $\pi$ -donor properties of these CSPs and hence the separation ability of **CSP-1** and **CSP-2** for  $\pi$ -acidic racemic enantiomers were expected. **CSP-2** has *pseudo*  $C_2$  symmetry;  $C_2$  symmetry is perturbed by the chlorine atom in the persubstituted benzene ring.

To our disappointment, both CSPs proved rather ineffective in separation of most test racemates (**TR 1–TR**

**23**) listed in Figure 7. The selected set of test racemates comprises a broad range of functionalities, from hydroxy, carbonyl, ether, ester, to amide group, polyaromatic and/or heterocyclic ring. These reference racemates were screened on the columns with most of the new CSPs reported in this review.

With some exceptions, nearly all well resolved racemates belong to *N*-3,5-dinitrobenzoyl (*N*-DNB) derivatives of  $\alpha$ -aminoacids isopropylesters (*N*-DNB- $\alpha$ -AA; **TR 16–TR 23**), Table II. They are also resolved by most

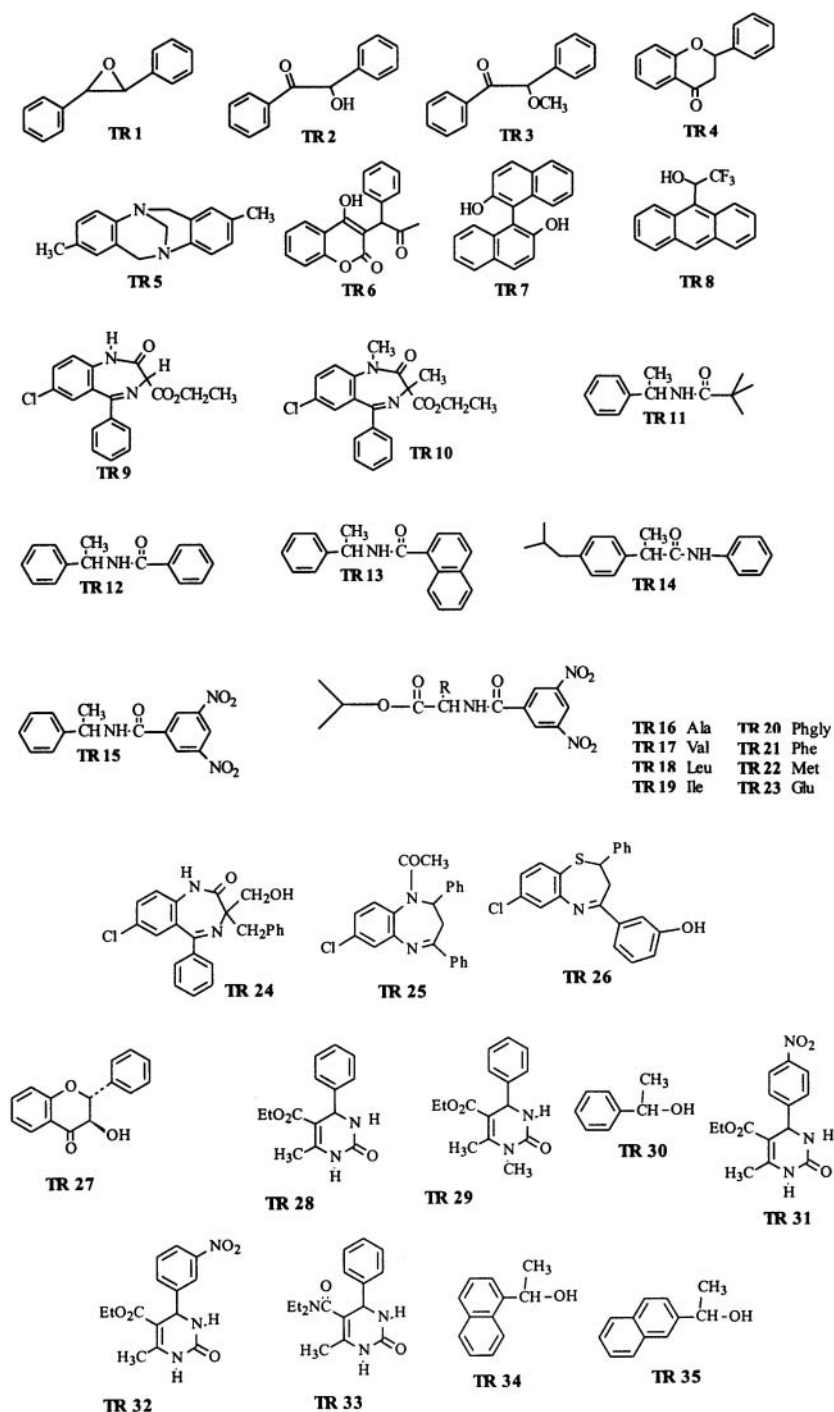


Figure 7. Test racemates **TR 1–TR 23**.<sup>35</sup>

TABLE II. HPLC results for the resolution of some solutes on the columns filled with stationary phases **CSP-1** and **CSP-2**.<sup>35</sup>

| Chiral stat. phase | Mobile phase <sup>(a)</sup> | Test rac.    | $k'_1$ | $\alpha$ | $R_S$ |
|--------------------|-----------------------------|--------------|--------|----------|-------|
| <b>CSP-1</b>       | B                           | <b>TR 6</b>  | 3.41   | 1.02     | 0.52  |
|                    | B                           | <b>TR 23</b> | 1.10   | 1.11     | 0.74  |
| <b>CSP-2</b>       | A                           | <b>TR 5</b>  | 2.08   | 1.05     | 0.50  |
|                    | A                           | <b>TR 7</b>  | 1.03   | 1.08     | 0.62  |
|                    | B                           | <b>TR 8</b>  | 1.53   | 1.01     | 0.31  |
|                    | B                           | <b>TR 15</b> | 4.74   | 1.05     | 0.92  |
|                    | A                           | <b>TR 19</b> | 1.05   | 1.16     | 0.62  |
|                    | A                           | <b>TR 20</b> | 2.05   | 1.06     | 0.54  |
| B                  | <b>TR 20</b>                | 1.55         | 1.03   | 0.28     |       |

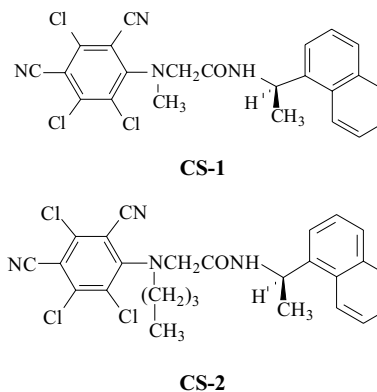
<sup>(a)</sup> A: n-Hexane/2-propanol (9:1);

B: n-Hexane/dichloromethane/methanol (10:3:0.1).

commercial N-DNB based CSPs,<sup>36</sup> and their interaction with chiral selectors is repeatedly studied.<sup>37,38</sup>

The results of enantioseparation revealed that selectors in **CSP-1** and **CSP-2** cannot form a sufficiently large molecular cleft, do not have an amide bond, and can only provide strong dipole-dipole, and weak  $\pi$ - $\pi$  interactions. We have therefore prepared compounds **CS-1** and **CS-2**, the pair of type **a**. chiral selectors, designed to form a large chiral hole. They are expected to contribute to enantioselection by hydrogen bonding *via* the CO-NH group and by  $\pi$ - $\pi$  interaction of the two  $\pi$ -basic units, Figure 8. In both selectors, the proton in the Ar-NH group is substituted by the hydrophobic alkyl group, derived either from sarcosine (Me) or introduced in a separate step (n-Bu), to avoid non-productive hydrogen bonding.

Using the standard procedure, these selectors are bound in the last step to Nucleosil 100-5 silica to form **CSP-3** and **CSP-4**, Scheme 4.

Figure 8. Structures of **CS-1** and **CS-2**.<sup>35</sup>

Representative examples of enantioseparation are given in Table III. Worth mentioning is the separation of the amides of a chiral  $\alpha$ -arylethylamine, **TR 12–TR 15**, on **CSP-3** rather than on **CSP-4**.

The difference in the enantioselectivity of these two CSPs indicated the importance of the dimen-

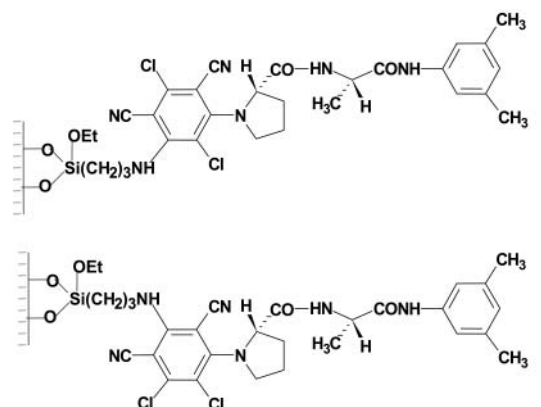
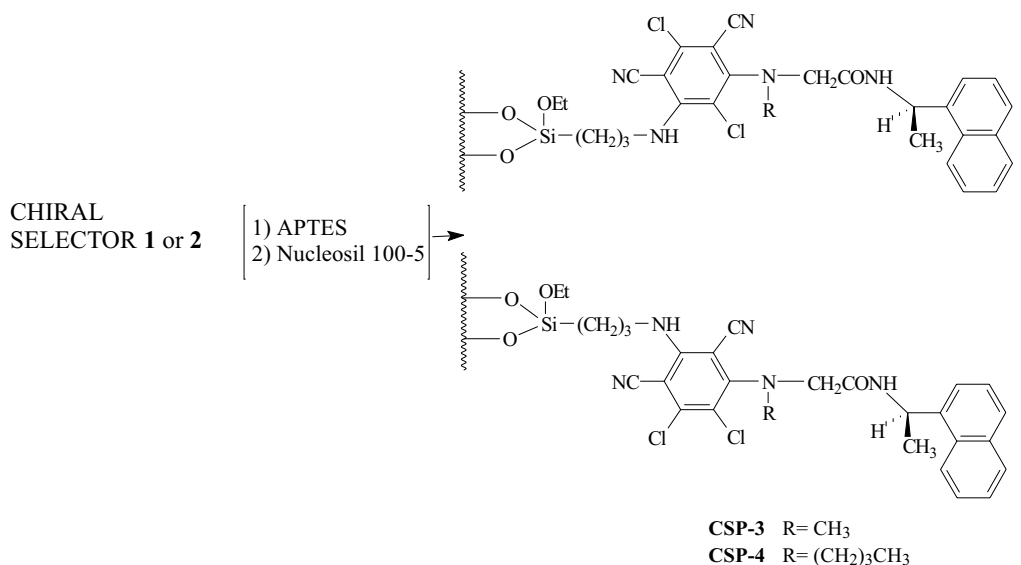
Figure 9. Structure of **CSP-5**.<sup>39</sup>Scheme 4. Preparation of **CSP-3** and **CSP-4**.<sup>35</sup>

TABLE III. HPLC results for the resolution of solutes **TR 1–TR 23** on the columns filled with stationary phases **CSP-3** and **CSP-4**.<sup>35</sup>

| CSP          | Mobile phase <sup>(a)</sup> | Test rac.    | $k'_1$ | $\alpha$ | $R_S$ |
|--------------|-----------------------------|--------------|--------|----------|-------|
| <b>CSP-3</b> | A                           | <b>TR 8</b>  | 1.65   | 1.06     | 0.52  |
|              | B                           | <b>TR 8</b>  | 2.52   | 1.05     | 0.55  |
|              | A                           | <b>TR 12</b> | 3.34   | 1.05     | 0.55  |
|              | B                           | <b>TR 14</b> | 1.14   | 1.05     | 0.91  |
|              | A                           | <b>TR 15</b> | 1.40   | 1.11     | 0.84  |
|              | A                           | <b>TR 16</b> | 2.91   | 2.14     | 4.92  |
|              | A                           | <b>TR 17</b> | 2.03   | 2.59     | 6.88  |
|              | A                           | <b>TR 18</b> | 5.19   | 2.09     | 7.29  |
|              | A                           | <b>TR 19</b> | 2.06   | 2.46     | 5.72  |
|              | A                           | <b>TR 21</b> | 6.23   | 1.70     | 5.68  |
|              | A                           | <b>TR 22</b> | 5.52   | 2.26     | 5.41  |
| <b>CSP-4</b> | A                           | <b>TR 14</b> | 0.26   | 1.07     | 0.89  |
|              | A                           | <b>TR 15</b> | 15.80  | 2.25     | 6.27  |
|              | A                           | <b>TR 16</b> | 5.34   | 1.96     | 4.74  |
|              | A                           | <b>TR 17</b> | 4.20   | 2.29     | 7.60  |
|              | A                           | <b>TR 18</b> | 3.91   | 1.98     | 5.28  |
|              | A                           | <b>TR 19</b> | 3.97   | 2.15     | 6.96  |
|              | A                           | <b>TR 21</b> | 9.63   | 1.66     | 3.96  |
|              | A                           | <b>TR 22</b> | 8.43   | 2.11     | 6.31  |
|              | A                           | <b>TR 23</b> | 5.00   | 1.80     | 3.58  |

(a) A: n-Hexane/2-propanol (9:1);

B: n-Hexane/dichloromethane/methanol (10:3:0.1).

sion of their chiral hole; in the latter case n-butyl chain presumably perturbs hydrogen bonding of the analyte to the amide carbonyl group, a crucial interaction involved in enantiorecognition.

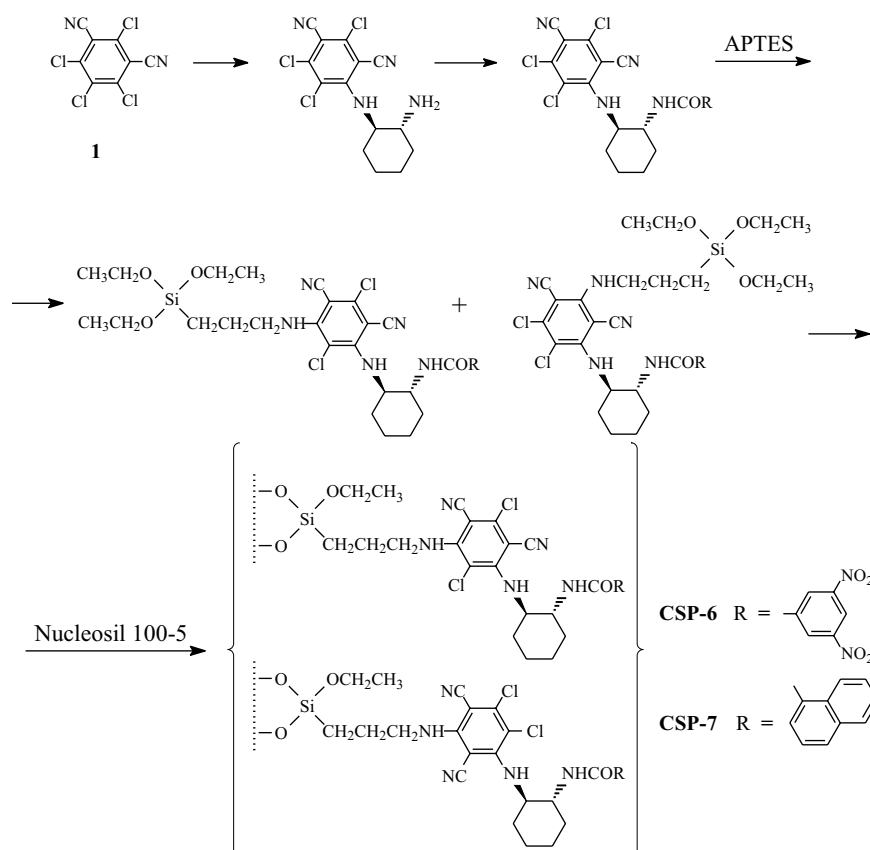
**CSP-5** with a broader resolution capacity was designed assuming that a larger chiral hole and two peptide bonds would contribute to better enantioselection, Figure 9.<sup>39</sup>

Dipeptide L-Pro-L-Ala unit and the strong  $\pi$ -donor 3,5-dimethylanilide (DMA) unit rendered **CSP-5** effective for the resolution of most **TRs** having the strong  $\pi$ -acceptor *N*-3,5-dinitrobenzoyl (*N*-DNB) unit.

However, at that point the problem of the resolution of most  $\pi$ -non-acidic **TRs** still remained unsolved. We therefore designed the next two CSPs, assuming that a more rigid but chiral cleft was required, which could be obtained from (1*R*,2*R*)-*trans*-diaminocyclohexane as a core chiral unit.<sup>40</sup> The first amino group was bound to persubstituted TCDCB, the second *via* an amide bond to the  $\pi$ -donor naphthoyl, or  $\pi$ -acceptor DNB group, Scheme 5.

To get some information about intramolecular interactions in the two chiral selectors, we performed the MM2 calculation on the model compounds **8** and **9**. Calculations revealed a completely different orientation of the two aromatic rings, Figure 10.

In the model compound **8**, the strong  $\pi$ -acidic DNB group and the slightly  $\pi$ -basic persubstituted benzene

Scheme 5. Preparation of **CSP-6** and **CSP-7**.<sup>40</sup>

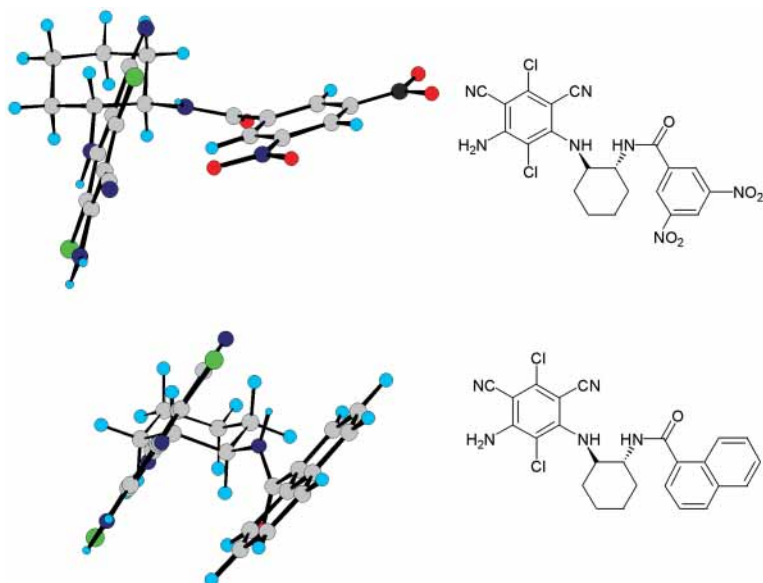


Figure 10. Ball and stick presentation of the lowest energy conformers of **8** and **9**.<sup>40</sup>

ring occupy T-shape or edge-to-face geometry, while in **9** the  $\pi$ -basic naphthyl group is oriented parallel (offset stacking) to the persubstituted benzene ring. It is reasonable to assume that two aromatic units in **CSP-6** and **CSP-7** easily »open up« to form a cleft when interacting with the chiral analyte. The results of enantioseparation with test racemates **TR 1–TR 23** are summarized in Table IV.

TABLE IV. Parameters obtained for enantioseparation of racemic analytes on columns filled with **CSP-6** and **CSP-7**.<sup>40, (a)</sup>

| CSP          | Mobile phase <sup>(b)</sup> | TR           | $k'_1$ | $\alpha$ | $R_S$               |
|--------------|-----------------------------|--------------|--------|----------|---------------------|
| <b>CSP-6</b> | A                           | <b>TR 6</b>  | 5.85   | 1.12     | 0.34                |
|              | A                           | <b>TR 9</b>  | 1.67   | 1.47     | 1.59                |
|              | A                           | <b>TR 11</b> | 1.14   | 1.51     | 1.34 <sup>(c)</sup> |
|              | A                           | <b>TR 12</b> | 9.35   | 1.08     | 0.35                |
|              | A                           | <b>TR 13</b> | 1.67   | 1.10     | 0.56                |
|              | A                           | <b>TR 14</b> | 1.39   | 1.20     | 0.79 <sup>(c)</sup> |
| <b>CSP-7</b> | B                           | <b>TR 6</b>  | 2.55   | 1.22     | 1.32                |
|              | B                           | <b>TR 9</b>  | 2.23   | 1.05     | 0.84                |
|              | B                           | <b>TR 15</b> | 4.75   | 1.13     | 0.99                |
|              | B                           | <b>TR 16</b> | 2.21   | 1.21     | 1.02                |
|              | B                           | <b>TR 17</b> | 2.01   | 1.07     | 0.53                |
|              | B                           | <b>TR 18</b> | 1.61   | 1.11     | 0.91                |
|              | B                           | <b>TR 20</b> | 2.97   | 1.20     | 1.57 <sup>(d)</sup> |
|              | B                           | <b>TR 21</b> | 2.80   | 1.05     | 0.32                |
|              | B                           | <b>TR 22</b> | 3.26   | 1.25     | 1.96                |
| B            | <b>TR 23</b>                | 2.26         | 1.24   | 2.04     |                     |

(a) Column dimension 150 × 4.6 ID mm, flow rate 1 ml / min.

(b) A: n-hexane/2-propanol (8:2); B: n-hexane/2-propanol (9:1).

(c) The *S*-enantiomer is eluted first.

(d) The *R*-enantiomer is eluted first.

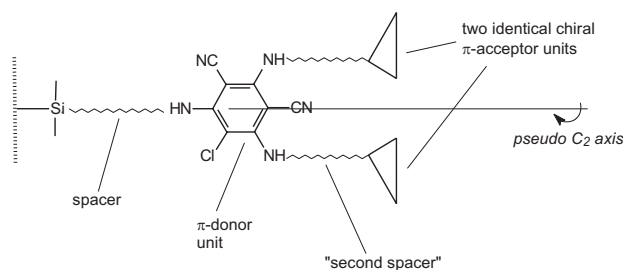


Figure 11. Schematic presentation of the structure of the tweezer-type CSPs with a »second spacer«.<sup>41</sup>

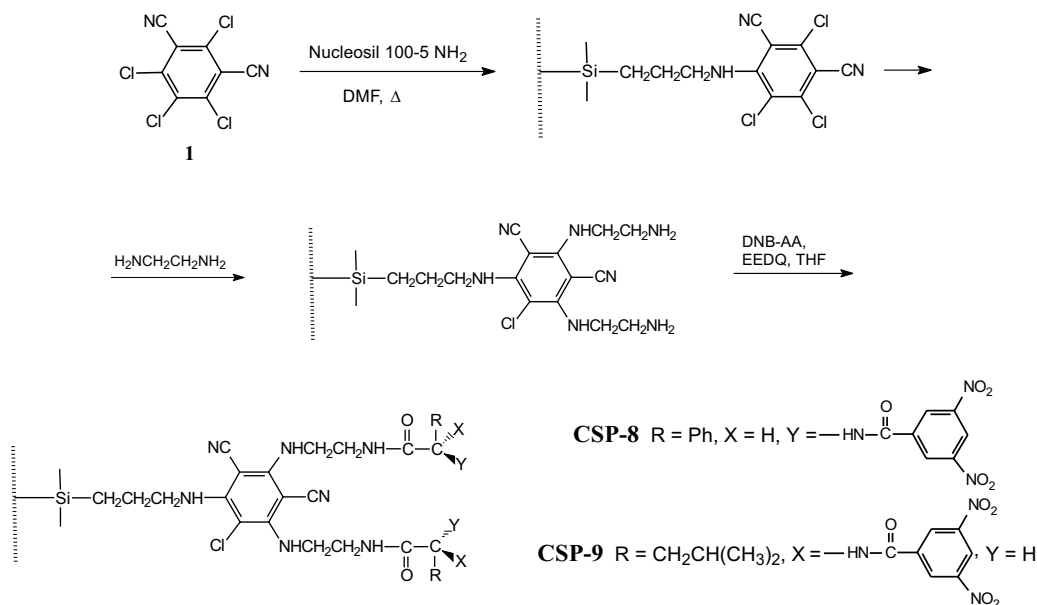
Both CSPs completely resolved **TR 6** and **TR 9**, analytes with a polyaromatic unit. The column with **CSP-6** did not resolve *N*-DNB-aminoacid esters **TR 16–TR 23**, which are usually well resolved. This selectivity indicated a limited ability of the designed cleft to receive larger molecules of racemic analytes. In the next step, we therefore prepared more conformationally flexible, *pseudo C<sub>2</sub>* symmetric, tweezer-type CSPs. Their overall structure is schematically presented in Figure 11.<sup>41</sup>

We had anticipated the »second spacer« between the branching unit and chiral selector, represented by an irregular triangle in Figure 11, and this concept was reduced to practice by preparing **CSP-8** and **CSP-9** according to Scheme 6.<sup>41</sup>

Nucleosil 100-5 NH<sub>2</sub> was used as the solid support, and  $\gamma$ -aminopropyl groups were exhaustively arylated by the excess of TCDCB in DMF. This solid phase was then reacted with excess of 1,2-diaminoethane to replace chlorines in 2- and 6-positions of the persubstituted ring, and in the final step terminal amino groups in the »second spacers« were acylated by DNB-D-PhGly and DNB-L-Leu, respectively.

Two HPLC columns filled with tweezer-type **CSP-8** and **CSP-9** were compared with the commercially avail-



Scheme 6. Preparation of the **CSP-8** and **CSP-9**.<sup>41</sup>

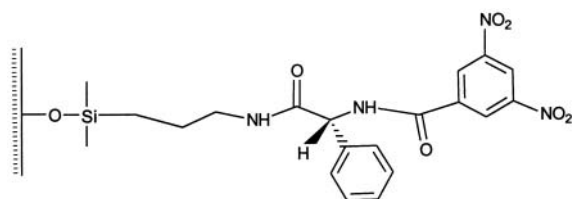
able column *Chiral II* from Macherey-Nagel, originally developed by Pirkle,<sup>42</sup> which contains CSP based on N-DNB-D-PhGly, Figure 12.

The results of enantioseparation of representative racemates are given in Table V.<sup>41</sup>

The results reveal that **CSP-8** and **CSP-9** fully match, and in some cases surpass the resolution efficacy of the commercial column *Chiral II*. An important quality of the columns filled with **CSP-8** and **CSP-9** is their higher loading capacity compared to *Chiral II*, revealing the enhanced capacity of the tweezer-type CSPs in Figure 2.

#### Column Enantiomerization on »Truncated« **CSP-8**

HPLC columns with stationary phase **CSP-9** have been commercialized in the USA under the name CHIRIS-AD2.<sup>43</sup> However, during the study of **CSP-9** preparation with a highly reproducible quality, an interesting phenomenon was observed. Separation of 3-carbomethoxy-1,4-benzodiazepine derivative **14** on some CHIRIS-AD2 columns was accompanied by a subtle difference in the peak shape, in some cases even by formation of a plateau between the two separated peaks, Figure 13a.<sup>44</sup> Since compound **14** has very acidic C(3)-H, flanked by three

Figure 12. CSP structure in the commercial *Chiral II* column.

double bonds, it was concluded that an »on-the-column enantiomerization«<sup>45,46</sup> process had taken place according to Scheme 7.

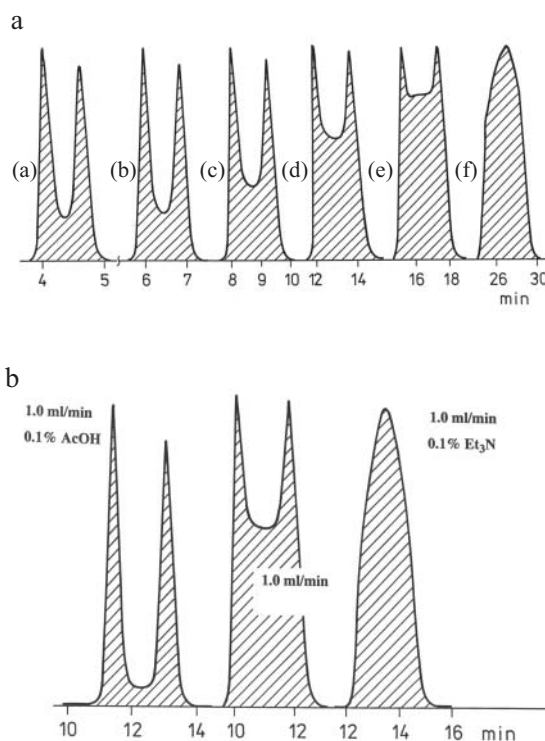


Figure 13. a) HPLC profiles of racemic **14** on **CSP-9**, eluted at 25 °C, with n-hexane/*i*-PrOH/MeOH (100:40:2), at various flow rates: (a) 3.0 ml/min, (b) 2.0 ml/min, (c) 1.5 ml/min, (d) 1.0 ml/min, (e) 0.8 ml/min, (f) 0.5 ml/min; b) Repeated resolution of racemic **14** on **CSP-9** by addition of 0.1 % AcOH and 0.1 % Et<sub>3</sub>N.<sup>44</sup>

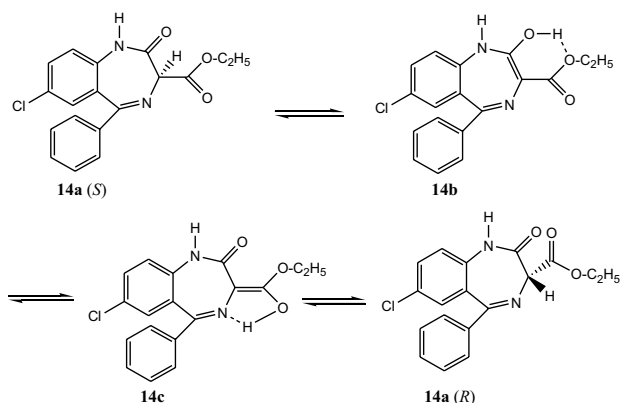
TABLE V. HPLC parameters obtained for racemates **TR 5–TR 22** with columns (150 mm × 4.6 mm ID) filled with **CSP-8** and **CSP-9** and commercial column *Chiral II* (250 mm × 4.0 mm ID)

| Rac.         | Mob.<br>phase <sup>(a)</sup> | $k_1'$ |       |                  | $\alpha$ |       |                  | $R_S$ |       |                  |
|--------------|------------------------------|--------|-------|------------------|----------|-------|------------------|-------|-------|------------------|
|              |                              | CSP-8  | CSP-9 | <i>Chiral II</i> | CSP-8    | CSP-9 | <i>Chiral II</i> | CSP-8 | CSP-9 | <i>Chiral II</i> |
| <b>TR 5</b>  | A                            | 1.51   | 1.20  | 1.55             | 1.13     | 1.00  | 1.34             | 0.58  | 0.00  | 1.82             |
|              | B                            | 0.80   | 0.65  | 1.07             | 1.12     | 1.00  | 1.00             | 0.75  | 0.00  | 0.00             |
| <b>TR 6</b>  | A                            | 11.46  | 6.20  | 4.33             | 1.27     | 1.25  | 1.39             | 0.72  | 0.33  | 1.80             |
|              | B                            | 11.76  | 16.03 | 5.60             | 1.17     | 1.24  | 1.29             | 2.26  | 1.87  | 3.21             |
| <b>TR 7</b>  | A                            | 3.57   | 2.89  | 1.99             | 1.29     | 1.22  | 1.51             | 1.33  | 0.37  | 2.09             |
|              | B                            | 5.95   | 6.77  | 4.66             | 1.30     | 1.26  | 1.47             | 2.41  | 2.10  | 3.50             |
| <b>TR 8</b>  | A                            | 23.46  | 16.49 | 14.15            | 1.19     | 1.19  | 1.28             | 0.85  | 0.45  | 1.33             |
|              | B                            | 33.22  | 7.77  | 1.23             | 1.20     | 4.74  | 1.00             | 1.71  | 6.03  | 0.00             |
| <b>TR 9</b>  | A                            | 3.84   | 2.67  | 3.67             | 1.05     | 1.00  | 1.12             | 0.53  | 0.00  | 1.05             |
|              | B                            | 1.04   | 0.69  | 10.31            | 1.00     | 1.00  | 1.23             | 0.00  | 0.00  | 1.73             |
| <b>TR 10</b> | A                            | 2.31   | 2.10  | 2.14             | 1.13     | 1.14  | 1.21             | 1.22  | 0.84  | 1.87             |
|              | B                            | 2.38   | 0.66  | 4.66             | 1.57     | 1.00  | 1.47             | 1.41  | 0.00  | 5.00             |
| <b>TR 11</b> | A                            | 8.24   | 7.60  | 6.15             | 1.15     | 1.00  | 1.26             | 1.35  | 0.00  | 2.04             |
|              | B                            | 0.80   | 3.15  | 3.64             | 1.00     | 1.00  | 1.00             | 0.00  | 0.00  | 0.00             |
| <b>TR 12</b> | A                            | 22.28  | 17.24 | 19.07            | 1.18     | 1.00  | 1.28             | 1.21  | 0.00  | 1.92             |
|              | B                            | 5.49   | 4.65  | 6.00             | 1.13     | 1.03  | 1.11             | 1.47  | 0.22  | 2.07             |
| <b>TR 13</b> | A                            | 3.28   | 2.67  | 2.50             | 1.15     | 1.06  | 1.26             | 1.30  | 0.28  | 1.64             |
|              | B                            | 1.49   | 0.71  | 0.96             | 1.00     | 1.29  | 1.00             | 0.00  | 0.24  | 0.00             |
| <b>TR 14</b> | A                            | 23.60  | 15.90 | 11.23            | 1.09     | 1.00  | 1.13             | 0.58  | 0.00  | 1.05             |
|              | B                            | 14.14  | 11.90 | 10.18            | 1.08     | 1.00  | 1.02             | 0.97  | 0.00  | 0.10             |
| <b>TR 15</b> | A                            | 11.26  | 7.44  | 6.48             | 1.18     | 1.50  | 1.11             | 1.12  | 1.02  | 1.09             |
|              | B                            | 7.80   | 6.95  | 4.86             | 1.18     | 1.56  | 1.16             | 2.02  | 4.75  | 2.12             |
| <b>TR 16</b> | A                            | 8.38   | 5.14  | 5.02             | 1.20     | 1.46  | 1.11             | 1.19  | 1.84  | 0.84             |
|              | B                            | 4.64   | 3.42  | 3.68             | 1.20     | 1.40  | 1.08             | 2.18  | 3.25  | 1.10             |
| <b>TR 17</b> | A                            | 7.42   | 4.29  | 4.47             | 1.16     | 1.56  | 1.00             | 1.02  | 1.94  | 0.00             |
|              | B                            | 5.70   | 3.80  | 3.65             | 1.18     | 1.65  | 1.07             | 2.35  | 4.66  | 0.91             |
| <b>TR 18</b> | A                            | 8.06   | 4.77  | 5.02             | 1.22     | 1.49  | 1.11             | 1.46  | 1.66  | 0.97             |
|              | B                            | 4.42   | 3.15  | 3.74             | 1.17     | 1.41  | 1.00             | 1.86  | 3.66  | 0.00             |
| <b>TR 19</b> | A                            | 14.43  | 8.76  | 7.39             | 1.26     | 1.39  | 1.20             | 1.60  | 1.57  | 1.62             |
|              | B                            | 7.67   | 5.30  | 5.14             | 1.27     | 1.35  | 1.22             | 3.32  | 2.83  | 2.55             |
| <b>TR 20</b> | A                            | 14.18  | 7.80  | 7.58             | 1.23     | 1.55  | 1.12             | 1.38  | 1.95  | 1.11             |
|              | B                            | 7.29   | 4.67  | 4.96             | 1.20     | 1.53  | 1.13             | 2.25  | 3.88  | 1.55             |
| <b>TR 21</b> | A                            | 18.17  | 10.23 | 9.40             | 1.21     | 1.52  | 1.12             | 1.28  | 3.44  | 1.08             |
|              | B                            | 10.46  | 6.69  | 6.71             | 1.21     | 1.55  | 1.14             | 2.33  | 5.16  | 1.80             |
| <b>TR 22</b> | A                            | 13.91  | 7.74  | 8.31             | 1.14     | 1.34  | 1.00             | 0.85  | 1.29  | 0.00             |
|              | B                            | 7.67   | 4.37  | 4.29             | 1.27     | 1.34  | 1.06             | 2.95  | 3.26  | 0.75             |

<sup>(a)</sup> A: n-Hexane/2-propanol (9:1); B: n-hexane/dichloromethane/methanol (100:30:1).

Analysis of the preparation protocol revealed that the column on which enantiomerization was observed, filled with **CSP-9**, was prepared with a lower excess of N-DNB- $\alpha$ -AA. This resulted in incomplete acylation of both 2-

aminoethylamino arms in the persubstituted intermediate, as shown in Figure 14. It was concluded that enantiomerization was base-catalyzed by non-acylated 2-aminoethylamino groups present in this CSP. In order to confirm

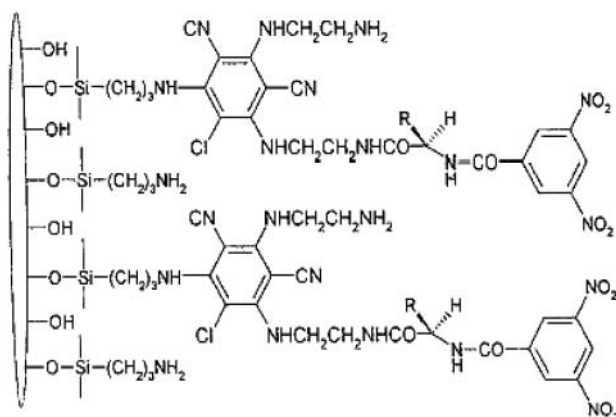
Scheme 7. Enantiomerization of compound **14**.<sup>44</sup>

base-catalysis as the origin of enantiomerization of **14**, we prepared a »truncated« **CSP-9** by using only 50 % mol of N-DNB-Leu.<sup>44</sup>

As expected, the larger proportion of free 2-aminoethylamino groups in the »truncated« **CSP-9** enhanced the enantiomerization rate. Figure 13 shows how the plateau between the two peaks of separated enantiomers increases with longer retention times.

From the slope obtained by plotting the log area (%) of the unreacted molecule zone (peaks) against the retention time, the first-order rate of enantiomerization can be estimated for the two enantiomers at 14.1 min<sup>-1</sup> and 22.2 min<sup>-1</sup>.<sup>44</sup>

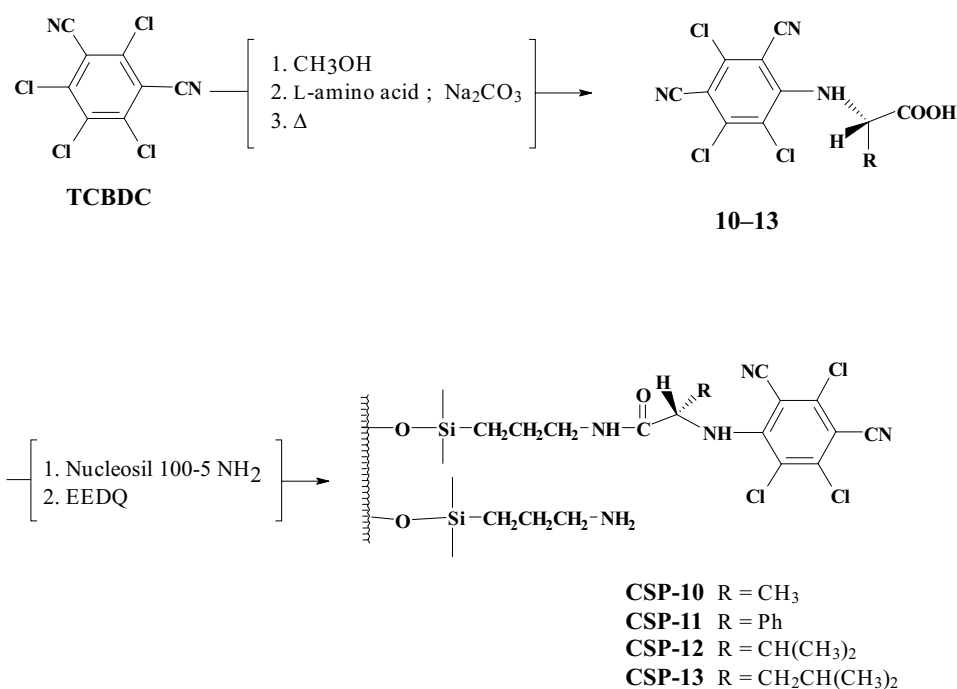
To further prove the role of the basic site in enantiomerization on **CSP-9**, resolution of racemic **14** was repeated by addition of 0.1 % AcOH and 0.1 % Et<sub>3</sub>N to the eluting solvent mixture, Figure 13b. Resolution was improved upon acid addition, while enantioseparation got completely lost upon the addition of amine!<sup>44</sup>

Figure 14. Schematic presentation of the »truncated« **CSP-9** (R=CH<sub>2</sub>CH(CH<sub>3</sub>)<sub>2</sub>).<sup>44</sup>

#### Brush-type CSPs with Persubstituted Benzene (TCDCB) as the Terminal Unit

The next set of CSPs proved to be particularly successful in separation of the commercially important class of racemic  $\alpha$ -aryloxypropionic acids. These columns are designed according to a simple concept. Persubstituted benzene ring as a terminal, highly polar aromatic unit is expected to enter a  $\pi$ - $\pi$ -type interaction with the  $\pi$ -donor aryloxy unit in analytes. This new class of CSPs **CSP-10–CSP-13** was prepared according to Scheme 8.<sup>47</sup>

Nucleophilic substitution of C(4) chlorine in TCDCB by the amino group of unprotected L-amino acids afforded *N*-aryl-AA derivatives **10–13**, which were bound to Nucleosil 100-5 NH<sub>2</sub> by the standard method. In Scheme 8 unacylated  $\gamma$ -aminopropyl residues are indicated; their

Scheme 8. Synthetic route for preparation of **CSP-10–CSP-13**.<sup>47</sup>

presence turned to be of crucial importance. It is known that up to 80–85 % of such unreacted groups are present in the Pirkle-type stationary phases.<sup>48</sup>

Screening of these CSPs has soon revealed their exceptional efficacy in separating representative racemic  $\alpha$ -aryloxypropionic acids (**TR 1/6–TR 20/6**), Tables VI and VII.

It was indicative that **CSP-10** exhibited the most effective enantioseparation. Bulkier substituents on the stereogenic center in **CSP-12** and **CSP-13** reduced the enantioseparation capacity, pointing to the importance of hydrogen bonding by the amide CO-N-H group of the selector.

TABLE VI. Structure of the analyzed racemic  $\alpha$ -aryloxypropionic acids<sup>47</sup>

| Test racemate  | R'                                | R   |
|----------------|-----------------------------------|---|
| <b>TR 1/6</b>  | H                                 | 2-CH <sub>3</sub> , 4-Cl                              |
| <b>TR 2/6</b>  | H                                 | 3-Cl  |
| <b>TR 3/6</b>  | H                                 | 3-C <sub>6</sub> H <sub>5</sub> CO                    |
| <b>TR 4/6</b>  | H                                 | 4-C <sub>6</sub> H <sub>5</sub> CO                    |
| <b>TR 5/6</b>  | H                                 | 2-C <sub>3</sub>                                      |
| <b>TR 6/6</b>  | H                                 | 3-C <sub>3</sub>                                      |
| <b>TR 7/6</b>  | H                                 | 4-C <sub>3</sub>                                      |
| <b>TR 8/6</b>  | H                                 | 4-CH <sub>2</sub> -CH <sub>3</sub>                    |
| <b>TR 9/6</b>  | H                                 | 2-Cl  |
| <b>TR 10/6</b> | H                                 | 2,5-(CH <sub>3</sub> ) <sub>2</sub>                   |
| <b>TR 11/6</b> | H                                 | 2,6-(CH <sub>3</sub> ) <sub>2</sub>                   |
| <b>TR 12/6</b> | H                                 | 4-C <sub>6</sub> H <sub>5</sub> CH <sub>2</sub>       |
| <b>TR 13/6</b> | H                                 | 4-(2,4-F <sub>2</sub> C <sub>6</sub> H <sub>3</sub> ) |
| <b>TR 14/6</b> | CH <sub>3</sub>                   | 3-CH <sub>3</sub>                                     |
| <b>TR 15/6</b> | CH <sub>3</sub>                   | 4-CH <sub>3</sub>                                     |
| <b>TR 16/6</b> | CH <sub>3</sub>                   | 2-Cl  |
| <b>TR 17/6</b> | -CH <sub>2</sub> -CH <sub>3</sub> | 2,6-(CH <sub>3</sub> ) <sub>2</sub>                   |
| <b>TR 18/6</b> | CH <sub>3</sub>                   | 4-(2,4-F <sub>2</sub> C <sub>6</sub> H <sub>3</sub> ) |
| <b>TR 19/6</b> |                                   |   |
| <b>TR 20/6</b> |                                   |   |

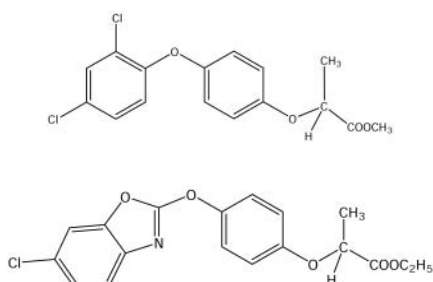


TABLE VII. HPLC resolution of **TR 1/6–TR 4/6** on **CSP-10** and **CSP-11**<sup>47,(a)</sup>

| Stationary phase | Test racemate | $k_1'$ | $\alpha$ | $R_S$ |
|------------------|---------------|--------|----------|-------|
| <b>CSP-10</b>    | <b>TR 1/6</b> | 0.63   | 1.43     | 1.28  |
|                  | <b>TR 2/6</b> | 4.35   | 1.16     | 1.35  |
|                  | <b>TR 3/6</b> | 4.74   | 1.11     | 0.96  |
|                  | <b>TR 4/6</b> | 6.13   | 1.21     | 1.26  |
| <b>CSP-11</b>    | <b>TR 1/6</b> | 8.03   | 1.11     | 0.76  |
|                  | <b>TR 2/6</b> | 5.53   | 1.07     | 0.88  |
|                  | <b>TR 3/6</b> | 12.18  | 1.03     | 0.63  |
|                  | <b>TR 4/6</b> | 3.87   | 1.12     | 0.54  |

(a) Mobile phase: n-hexane/2-propanol/acetic acid (90 : 9 : 1).

Figure 15 shows that the first eluted enantiomer of selected racemates **TR 6/6** and **TR 13/6** has a negative CD band at 254 nm and the second eluted enantiomers a positive one.

It was previously reported that the CD spectra of (*S*)-enantiomers of 2-aryloxypropionic acids are characterized by the negative CD band in the region 240–300 nm.<sup>49</sup> Consequently, the faster running enantiomers on our CSPs have (*S*)-configuration whereas (*R*)-enantiomers are more strongly bound. In this case, the original concept of enantio-recognition, as presented in Figure 1, is obeyed; CSPs based on (*S*)-amino acid derivatives bound more strongly (*R*)-enantiomers of  $\alpha$ -aryloxypropionic acids.

When in the mobile phase n-hexane/2-propanol/AcOH (98:2:0.2) trifluoroacetic acid (TFA) was substituted for acetic acid, resolution was completely eliminated. This observation, along with poor resolution of the correspond-

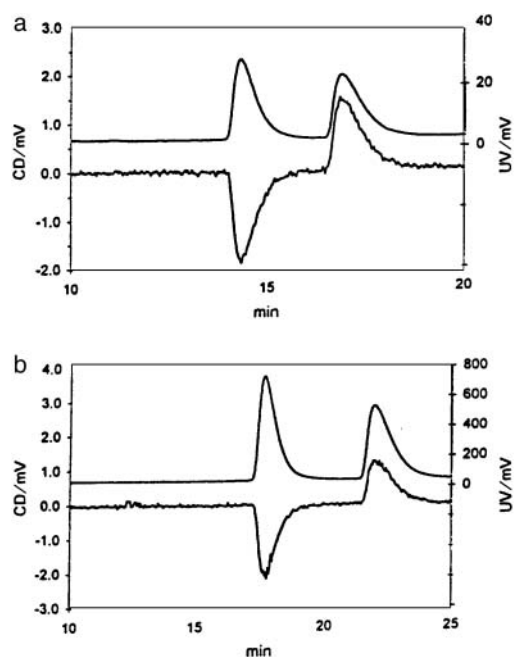
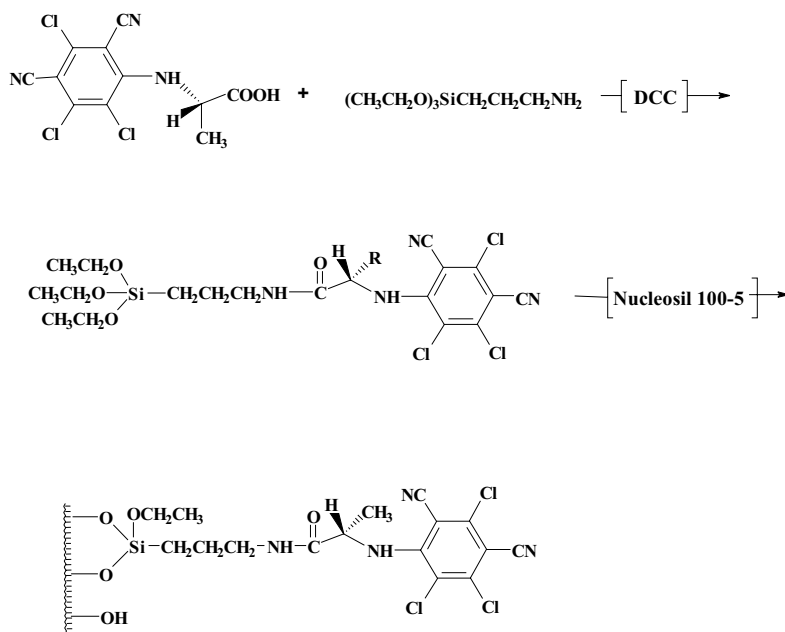
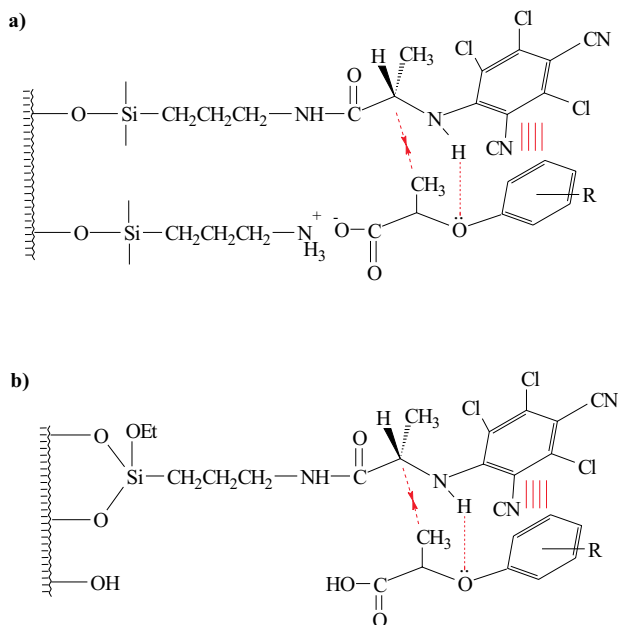


Figure 15. HPLC resolution of samples **TR 6/6** (a) and **TR 13/6** (b), monitored by simultaneous UV and CD detection at 254 nm.<sup>47</sup>

Scheme 9. Preparation of **CSP-14**.<sup>47</sup>

ing Me-esters of  $\alpha$ -aryloxypropionic acids revealed the importance of the acid–base interaction in enantioselection. Namely, the low coverage density of **CSP-10**, calculated as 0.38 groups/nm<sup>2</sup> of the specific surface area of silica gel,<sup>47</sup> suggested the specific role of unreacted  $\gamma$ -aminopropyl groups in the enantioselection process. Rather strong aryloxypropionic acids ( $pK_a$  3.2–3.4)<sup>50</sup> protonate the residual primary amino groups of the spacer, which enables the »anchor and align« interaction with the molecules of the analyte when they approach the chiral selector. This proton transfer is completely suppressed when strong TFA is added.

Figure 16. Possible chiral recognition mechanism for resolution of  $\alpha$ -aryloxypropionic acids on **CSP-10** (a) and **CSP-14** (b).<sup>47</sup>**CSP-14**

In order to provide further evidence in support of this hypothesis, **CSP-14** was prepared by the route presented in Scheme 9.<sup>47</sup>

**CSP-14** contains the same chiral selector as **CSP-10**, but has no unreacted  $\gamma$ -aminopropyl groups on the silica surface. As can be seen from Table VIII, this CSP exhibits very low chiral separation of the four selected racemic  $\alpha$ -aryloxy propionic acids.

All these data suggest the mechanism of enantioselection presented in Figure 16.

In the case of **CSP-10**, cumulative interaction seems to include formation of ion pairs (Coulombic interactions) between the selectand carboxylic groups and residual unreacted  $\gamma$ -aminopropyl groups on silica. Be-

TABLE VIII. HPLC parameters obtained for enantioseparation of **TR 1/6–4/6** on columns filled with stationary phases **CSP-14** and **CSP-10**.<sup>47,(a)</sup>

| Stationary phase | Test racemate | $k_1'$ | $\alpha$ | $R_S$             |
|------------------|---------------|--------|----------|-------------------|
| <b>CSP-14</b>    | <b>TR 1/6</b> | 0.59   | 1        | –                 |
|                  | <b>TR 2/6</b> | 0.74   | 1.02     | nm <sup>(b)</sup> |
|                  | <b>TR 3/6</b> | 0.61   | 1        | –                 |
|                  | <b>TR 4/6</b> | 0.66   | 1.03     | 0.54              |
| <b>CSP-10</b>    | <b>TR 1/6</b> | 0.63   | 1.43     | 1.28              |
|                  | <b>TR 2/6</b> | 4.35   | 1.16     | 1.35              |
|                  | <b>TR 3/6</b> | 4.74   | 1.11     | 0.96              |
|                  | <b>TR 4/6</b> | 6.13   | 1.21     | 1.26              |

(a) Mobile phase: 98% n-hexane/2-propanol (8:2) / 2% acetic acid (vol.); flow 1 ml min<sup>-1</sup>.

(b) nm = not measurable.

sides,  $\pi$ - $\pi$  interactions between the  $\pi$ -acid persubstituted benzene ring and the  $\pi$ -basic oxyaromatic ring in the selectand, hydrogen bonding from the amide group in CSP to etheral oxygen atom in the selectand, and van der Waals (VDW) interactions between the groups on the chiral center contribute to enantioselectivity. To the best of our knowledge, this is the first example in which an achiral unit on silica was directly involved in the process of chiral recognition. This case resembles the recently demonstrated positive effect on enantioselectivity of an achiral ligand in a chiral, catalytic organometallic complex; the authors define this effect as »achiral amplification of chiral environment«.<sup>51</sup>

### CSPs Containing Tetrasubstituted Benzene (CDNB) as the Branching Unit

As repeatedly stated,  $\pi$ - $\pi$  interactions between the chiral selector and solute enantiomers are of prime importance for enantioselectivity.

Continuing the project of novel CSPs, we have re-examined our selection of TCDCB as the branching unit, which is highly polar but void of  $\pi$ -acidity. Accumulated experience, however, has revealed the utmost importance of the  $\pi$ -acidic component in the selector for enantioselectivity of a vast number of  $\pi$ -basic analytes.<sup>52,53</sup>

In general, interactions between aromatic molecules constitute an important class of intermolecular forces in chemistry, biology and materials science. Aromatic  $\pi$ - $\pi$  interactions control a series of molecular recognition and self-assembly phenomena, enantioselectivity and enantioseparation among them. These interactions are described by some well known models developed after 1990 by Saunders and Hunter.<sup>54,55</sup> These authors have demonstrated that the face-to-face stacked orientation maximizes  $\pi$ -elec-

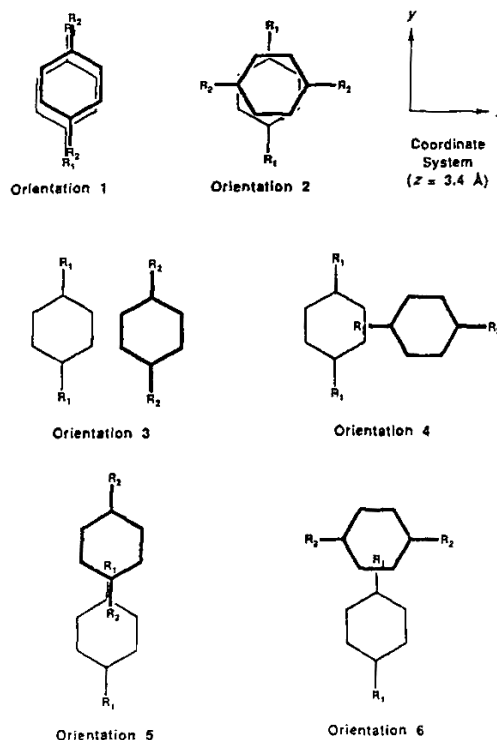
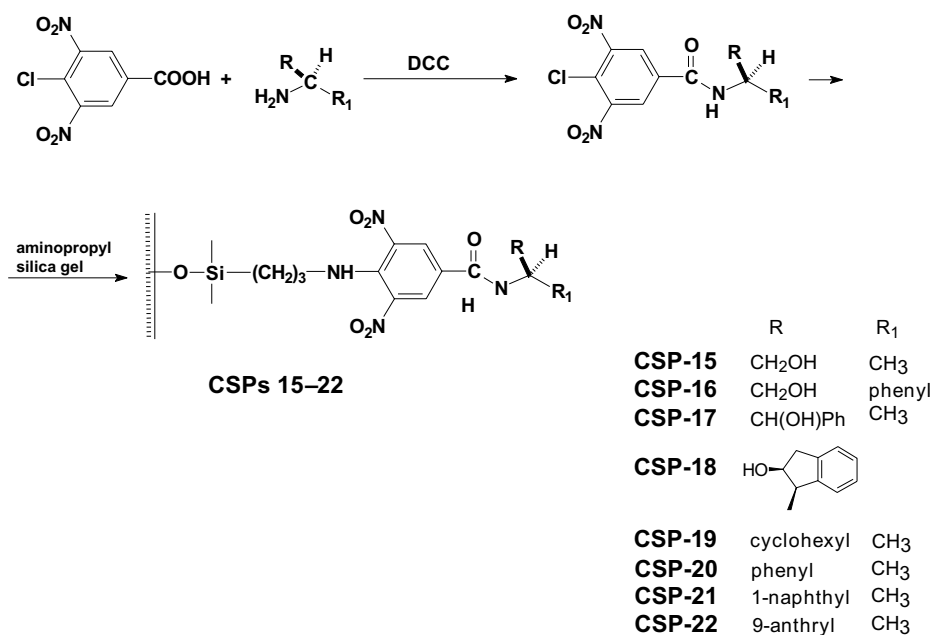


Figure 17. Orientation for the  $\pi$ - $\pi$  interactions between polarized  $\pi$ -systems;  $R_1$  and  $R_2$  are the polarizing groups.<sup>54</sup>

tron repulsion, whereas for the offset stacked orientation, and in particular the edge-to-face orientation, attractive interactions between the positively charged  $\sigma$ -framework and negatively charged  $\pi$ -electrons prevail. Thus,  $\pi$ -stacking is associated with large repulsive electrostatic interactions and is therefore much less favorable than it was argued for a long time on the basis of VDW interactions and solvophobic effects.



Scheme 10. Preparation of **CSP-15–CSP-22**.<sup>56</sup>

TABLE IX. Results of the evaluation of HPLC columns filled with **CSPs 15–18**<sup>56, (a)(b)</sup>

| Analyte      | CSP-15 |          |       | CSP-16 |          |       | CSP-17 |          |       | CSP-18 |          |       |
|--------------|--------|----------|-------|--------|----------|-------|--------|----------|-------|--------|----------|-------|
|              | $k'_2$ | $\alpha$ | $R_S$ | $k'_2$ | $\alpha$ | $R_S$ | $k'_2$ | $\alpha$ | $R_S$ | $k'_2$ | $\alpha$ | $R_S$ |
| <b>TR 2</b>  | 0.19   | 1.0      | 0     | 2.12   | 1.04     | nm    | 0.25   | 1.0      | 0     | 2.41   | 1.06     | 0.32  |
| <b>TR 5</b>  | 1.16   | 1.0      | 0     | 1.41   | 1.0      | 0     | 1.33   | 1.0      | 0     | 1.47   | 1.12     | 0.79  |
| <b>TR 9</b>  | 9.79   | 1.07     | nm    | 36.02  | 1.0      | 0     | 11.92  | 1.0      | 0     | 44.41  | 1.17     | 0.86  |
| <b>TR 12</b> | 2.98   | 1.0      | 0     | 4.25   | 1.09     | 0.89  | 4.14   | 1.0      | 0     | 3.33   | 1.07     | 0.59  |
| <b>TR 16</b> | 4.03   | 1.05     | 0.73  | 8.12   | 1.15     | 1.34  | 5.73   | 1.07     | 0.93  | 7.81   | 1.20     | 2.09  |
| <b>TR 17</b> | 1.56   | 1.02     | nm    | 3.48   | 1.11     | 0.83  | 2.95   | 1.0      | 0     | 4.15   | 1.17     | 2.40  |
| <b>TR 18</b> | 2.31   | 1.12     | 0.54  | 5.12   | 1.07     | 0.41  | 3.76   | 1.07     | 0.91  | 5.26   | 1.25     | 1.45  |
| <b>TR 19</b> | 1.53   | 1.24     | 0.90  | 3.34   | 1.05     | 0.29  | 2.79   | 1.12     | 0.79  | 3.71   | 1.22     | 2.16  |
| <b>TR 20</b> | 2.50   | 1.05     | 0.36  | 6.54   | 1.18     | 1.60  | 4.34   | 1.04     | 0.51  | 6.36   | 1.14     | 1.54  |
| <b>TR 21</b> | 2.34   | 1.07     | 0.47  | 6.04   | 1.11     | 0.86  | 4.20   | 1.06     | 0.71  | 6.34   | 1.23     | 2.30  |
| <b>TR 22</b> | 4.07   | 1.05     | 0.68  | 8.64   | 1.07     | 0.48  | 6.26   | 1.08     | 0.96  | 9.12   | 1.21     | 2.38  |
| <b>TR 23</b> | 3.17   | 1.0      | 0     | 5.20   | 1.08     | 0.44  | 3.95   | 1.07     | 0.88  | 5.87   | 1.16     | 1.80  |

(a) Column dimensions 250 mm × 4.6 mm ID; mobile phase n-hexane/dichloromethane/2-propanol (100:30:1); flow 1.0 ml min<sup>-1</sup>.

(b) nm = not measurable.

TABLE X. Results of the evaluation of HPLC columns filled with **CSPs 19–22**<sup>56, (a)</sup>

| Analyte      | CSP-19 |          |       | CSP-20 |          |       | CSP-21 |          |       | CSP-22 |          |       |
|--------------|--------|----------|-------|--------|----------|-------|--------|----------|-------|--------|----------|-------|
|              | $k_1$  | $\alpha$ | $R_S$ | $k_1$  | $\alpha$ | $R_S$ | $k_1$  | $\alpha$ | $R_S$ | $k_1$  | $\alpha$ | $R_S$ |
| <b>TR 8</b>  | 0.44   | 1.0      | 0     | 0.43   | 1.0      | 0     | 0.27   | 1.0      | 0     | 0.94   | 1.05     | 0.21  |
| <b>TR 10</b> | 0.97   | 1.0      | 0     | 0.81   | 1.0      | 0     | 0.78   | 1.07     | 0.82  | 1.41   | 1.10     | 0.42  |
| <b>TR 11</b> | 3.00   | 1.0      | 0     | 0.89   | 1.11     | 0.68  | 0.53   | 1.17     | 0.92  | 1.44   | 1.10     | 1.02  |
| <b>TR 12</b> | 2.04   | 1.0      | 0     | 1.79   | 1.11     | 0.95  | 1.83   | 1.11     | 1.07  | 4.58   | 1.10     | 0.65  |
| <b>TR 13</b> | 4.12   | 1.0      | 0     | 3.59   | 1.11     | 1.48  | 3.12   | 1.07     | 0.66  | 2.63   | 1.12     | 0.24  |
| <b>TR 14</b> | 0.87   | 1.0      | 0     | 0.74   | 1.09     | 0.52  | 0.61   | 1.09     | 0.57  | 1.76   | 1.11     | 1.10  |
| <b>TR 15</b> | 1.79   | 1.0      | 0     | 2.46   | 1.13     | 1.17  | 4.63   | 1.46     | 4.20  | 1.67   | 1.19     | 0.22  |
| <b>TR 16</b> | 1.05   | 1.0      | 0     | 1.17   | 1.11     | 0.92  | 1.50   | 1.36     | 2.08  | 5.55   | 1.05     | 0.52  |
| <b>TR 17</b> | 0.87   | 1.0      | 0     | 0.93   | 1.19     | 1.17  | 1.33   | 1.62     | 3.80  | 4.53   | 1.15     | 1.47  |
| <b>TR 18</b> | 0.74   | 1.0      | 0     | 0.79   | 1.27     | 1.41  | 1.11   | 1.79     | 4.00  | 3.31   | 1.17     | 2.00  |
| <b>TR 19</b> | 1.15   | 1.0      | 0     | 0.89   | 1.20     | 1.32  | 1.29   | 1.61     | 3.31  | 4.31   | 1.12     | 0.81  |
| <b>TR 20</b> | 1.17   | 1.0      | 0     | 1.54   | 1.0      | 0     | 2.99   | 1.26     | 2.33  | 9.97   | 1.09     | 0.96  |
| <b>TR 22</b> | 1.37   | 1.0      | 0     | 1.50   | 1.20     | 1.44  | 2.24   | 1.59     | 4.35  | 8.52   | 1.12     | 1.35  |
| <b>TR 27</b> | 0.79   | 1.0      | 0     | 0.98   | 1.0      | 0     | 0.38   | 1.0      | 0     | 1.37   | 1.25     | 1.35  |

(a) Column dimensions 250 mm × 4.6 mm ID; mobile phase n-hexane/2-propanol (8:2); flow rate 1.0 ml min<sup>-1</sup>.

Interaction between two aromatic systems polarized by heteroatoms or groups is of particular importance for enantioselectivity. Hunter has proposed six main orientations for the stacked offset  $\pi$ - $\pi$  interactions between achiral, polarized  $\pi$ -systems, Figure 17.<sup>54</sup>

The most important implication of the  $\pi$ -polarization effect in the field of molecular enantioselectivity is redefinition of the electron-donor acceptor (EDA) concept. The simple EDA concept is misleading since every molecule includes both electron-rich or donor and electron-poor or acceptor regions. The net intermolecular interaction depends on the way such regions are aligned.

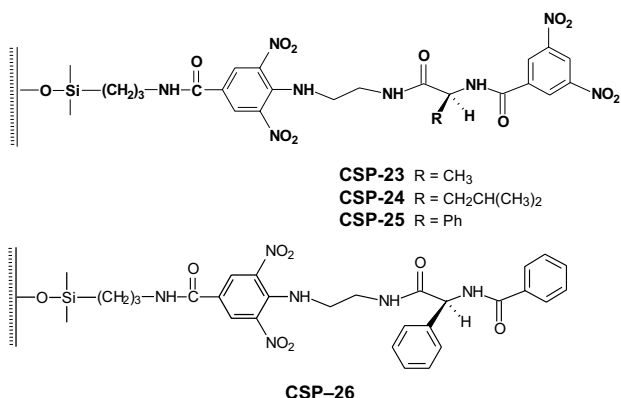
Having these arguments in mind, we selected the commercially available 4-chloro-3,5-dinitro benzoic acid (CDNB) as the branching unit for our next studies. CDNB

offers type **a**. branching; however, its  $\pi$ -acidity is high, and it was expected to significantly contribute to the enantioselectivity process.

The first group of chiral stationary phases with this unit were prepared according to Scheme 10.<sup>56</sup>

In the **CSP-15–CSP-18**, 1,2-amino alcohols are present as chiral selectors, while chiral amines have taken over this function in **CSP-19–CSP-22**. Most of these CSPs exhibited rather low enantioselectivity in resolution of the standard set of test racemates, Figure 7.

Comparative tests of their separation efficacy revealed the important contribution of the  $\pi$ -acidic branching unit, amide group of 3,5-dinitro-4-alkylaminobenzoic acid, but a limited contribution of both the hydrophilic hydroxy group in **CSP-15–CSP-18** and the  $\pi$ -basic aromatic unit in **CSP-19–CSP-22**, Tables IX and X.

Figure 18. Schematic presentation of **CSPs 23–26**.<sup>57</sup>

The results given in Tables IX and X suggest replacement of the chiral selectors with  $\pi$ -basic units by the selectors with the second, strong  $\pi$ -acid unit. We have therefore recently started a study of **CSP-23–CSP-25** (Figure 18) containing a »second spacer« 1,2-diaminoethane, and N-DNB- $\alpha$ -AA as the  $\pi$ -acid chiral selector unit.<sup>57</sup>

These CSPs are conceptually related to **CSP-8** and **CSP-9**, in that they have the »second spacer« and chiral selector in common. They exhibit nearly the same enantioseparation factors. To test the relative contribution of the  $\pi$ - $\pi$  interaction between the  $\pi$ -acid selector and  $\pi$ -acid racemic selectand *vs.* the interaction between the  $\pi$ -acid selector but  $\pi$ -basic racemic selectand, we have prepared two series of test racemates, Figure 19.<sup>57</sup>

Both are derivatives of isopropyl esters of  $\alpha$ -AA, the first group having the *N*-benzoyl (*N*-B) group and the second the *N*-DNB group.

To confirm the predominant contribution to enantioseparation of the matching  $\pi$ -acceptor groups in **CSP** and in **TR**, and to demonstrate the minor importance of the matching weak  $\pi$ -donor (or  $\pi$ -neutral) groups in the selector and selectand, we have prepared **CSP-26**, which comprises the  $\pi$ -neutral *N*-B unit in the chiral selector.<sup>57</sup>

The column with **CSP-26** proved almost ineffective for  $\pi$ -basic **TR 1/I–TR 7/I**, and, with one exception, partially effective in separation of **TR 1A/I–TR 7A/I**. These results clearly reveal the importance of the  $\pi$ - $\pi$  acid interaction between two electron deficient species, and limited contribution of the  $\pi$ - $\pi$  interaction between two  $\pi$ -neutral species.

The results are summarized in Table XI, where distribution of the average  $\alpha$ -value shows a much higher

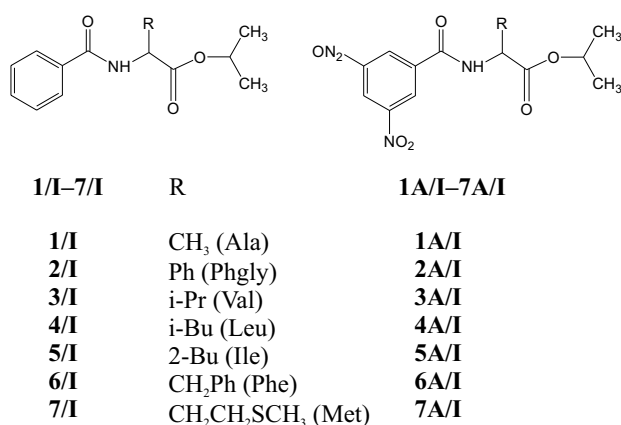
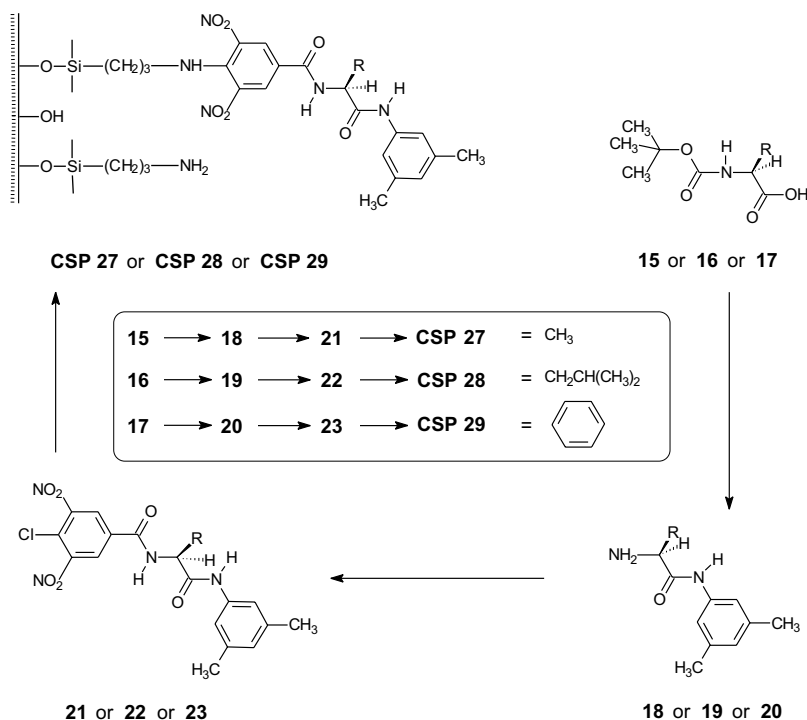
Figure 19. Test racemates **TR 1/I–TR 7/I** and **TR 1A/I–TR 7A/I**.<sup>57</sup>Scheme 11. Preparation of chiral stationary phases **CSP-27–CSP-29**.<sup>59</sup>



TABLE XI.  $\pi$ -Electron character of the interacting aromatic groups on **CSP-23–CSP-26** and **TR 1/I–TR 7/I**, and **TR 1A/I–TR 7A/I**, and their separation factors ( $\alpha$ )<sup>57</sup>

| $\pi$ -character of interacting groups |                              | min. $\alpha$ –max. $\alpha$ | $\alpha$ (average) |
|--|------------------------------|------------------------------|--------------------|
| <b>CSP-23, 24, 25</b><br>acceptor      | <b>1A/I–7A/I</b><br>acceptor | 1.12–1.48                    | 1.27               |
| <b>CSP-23, 24, 25</b><br>acceptor      | <b>1/I–7/I</b><br>neutral    | 1.00–1.62                    | 1.20               |
| <b>CSP-26</b><br>neutral               | <b>1A/I–7A/I</b><br>acceptor | 1.00–1.26                    | 1.19               |
| <b>CSP-26</b><br>neutral               | <b>1/I–7/I</b><br>neutral    | 1.00–1.06                    | 1.03               |

enantioseparation ability of the systems (TR-CSP) where both contain  $\pi$ -acceptor units than those comprising a  $\pi$ -acceptor within the selector or analyte. When neutral  $\pi$ -systems are present in both selector and analyte, only poor enantioselectivity was observed. This is the first

experimental demonstration of relative contributions of the two types of  $\pi$ -electron containing groups, acid and basic or  $\pi$ -donors and  $\pi$ -acceptors, to enantioselectivity on CSPs.

#### *CSPs Specifically Designed for Enantioselective Separation of Dihydropyrimidones*

Prompted by the observation that **CSP-23–CSP-26**, based on the 3,5-dinitrobenzoic amide bound in *para*-position to  $\gamma$ -aminopropyl silica, have efficiently separated racemic 4-aryl-dihydropyrimidone (DHPM) derivatives, compounds of significant pharmacological importance because of their antihypertensive activity,<sup>58</sup> we have designed CSPs specifically intended for separation of this class of racemates, Scheme 11.<sup>59</sup>

This novel chiral packing material was prepared by bonding to  $\gamma$ -aminopropyl silica 3,5-dimethylanilides (DMA) of some representative N-DNB derivatives of  $\alpha$ -amino acids; L-Ala, L-Val, L-Leu and L-PheGly. The

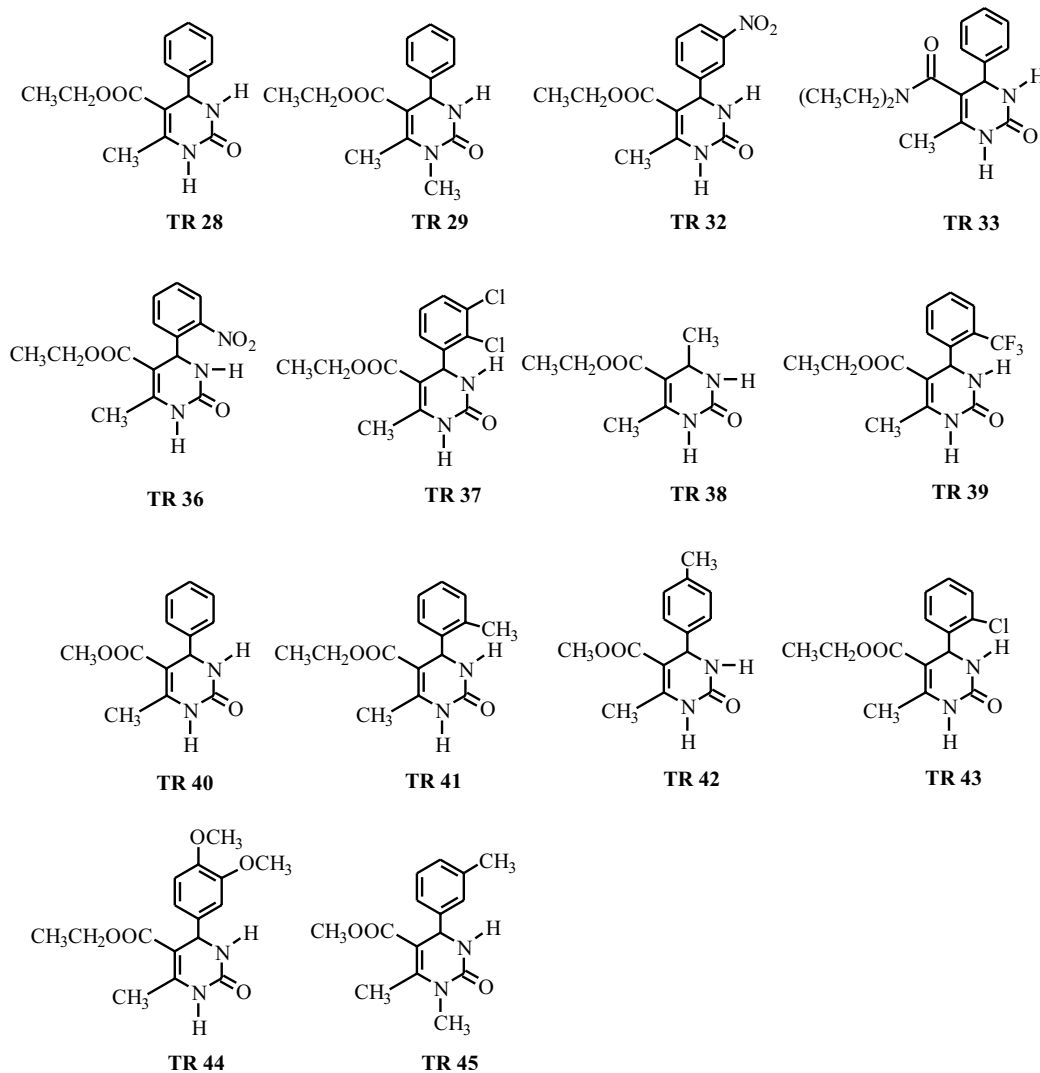


Figure 20. 3,4-Dihydro-2(1H)-pyrimidone racemates used for **CSP-27–CSP-29** evaluation.

TABLE XII. Results obtained for enantioseparation of racemic analytes listed in Figure 20 on the columns filled with chiral stationary phases **CSP-27–CSP-29**<sup>59</sup>, (a)

| Racemic analyte | <b>CSP-27</b> |          |       | <b>CSP-28</b> |          |       | <b>CSP-29</b> |          |       |
|-----------------|---------------|----------|-------|---------------|----------|-------|---------------|----------|-------|
|                 | $k'_1$        | $\alpha$ | $R_S$ | $k'_1$        | $\alpha$ | $R_S$ | $k'_1$        | $\alpha$ | $R_S$ |
| <b>TR 28</b>    | 4.26          | 1.18     | 2.19  | 2.90          | 1.31     | 3.28  | 4.87          | 1.21     | 2.61  |
| <b>TR 29</b>    | 3.11          | 1.18     | 2.08  | 2.06          | 1.21     | 1.80  | 3.50          | 1.17     | 1.63  |
| <b>TR 32</b>    | 9.31          | 1.23     | 3.22  | 6.15          | 1.39     | 3.02  | 10.92         | 1.21     | 2.37  |
| <b>TR 33</b>    | 16.47         | 1.00     | 0.00  | 12.92         | 1.08     | 0.94  | 22.82         | 1.07     | 0.97  |
| <b>TR 36</b>    | 8.12          | 1.14     | 1.51  | 5.51          | 1.31     | 3.88  | 9.45          | 1.13     | 1.82  |
| <b>TR 37</b>    | 4.32          | 1.10     | 0.96  | 2.66          | 1.18     | 1.46  | 5.26          | 1.11     | 0.93  |
| <b>TR 38</b>    | 4.70          | 1.18     | 1.71  | 2.91          | 1.25     | 1.68  | 5.73          | 1.24     | 1.65  |
| <b>TR 39</b>    | 2.81          | 1.10     | 0.93  | 1.77          | 1.22     | 1.34  | 3.23          | 1.12     | 0.99  |
| <b>TR 40</b>    | 5.40          | 1.20     | 1.84  | 3.25          | 1.27     | 2.02  | 6.21          | 1.24     | 1.79  |
| <b>TR 41</b>    | 4.58          | 1.14     | 1.21  | 2.73          | 1.27     | 1.65  | 5.45          | 1.24     | 1.67  |
| <b>TR 42</b>    | 3.43          | 1.04     | 0.31  | 2.15          | 1.06     | 0.67  | 3.93          | 1.08     | 0.89  |
| <b>TR 43</b>    | 4.01          | 1.10     | 0.92  | 2.47          | 1.21     | 1.58  | 4.61          | 1.13     | 0.93  |
| <b>TR 44</b>    | 16.26         | 1.36     | 3.12  | 9.00          | 1.52     | 3.38  | 21.23         | 1.28     | 2.00  |
| <b>TR 45</b>    | 4.48          | 1.18     | 1.62  | 2.73          | 1.26     | 1.85  | 4.96          | 1.20     | 1.63  |

(a) Column dimensions 250 mm x 4.6 mm ID; n-hexane/2-propanol/acetic acid (180:20:1); flow rate 2.0 ml min<sup>-1</sup>.

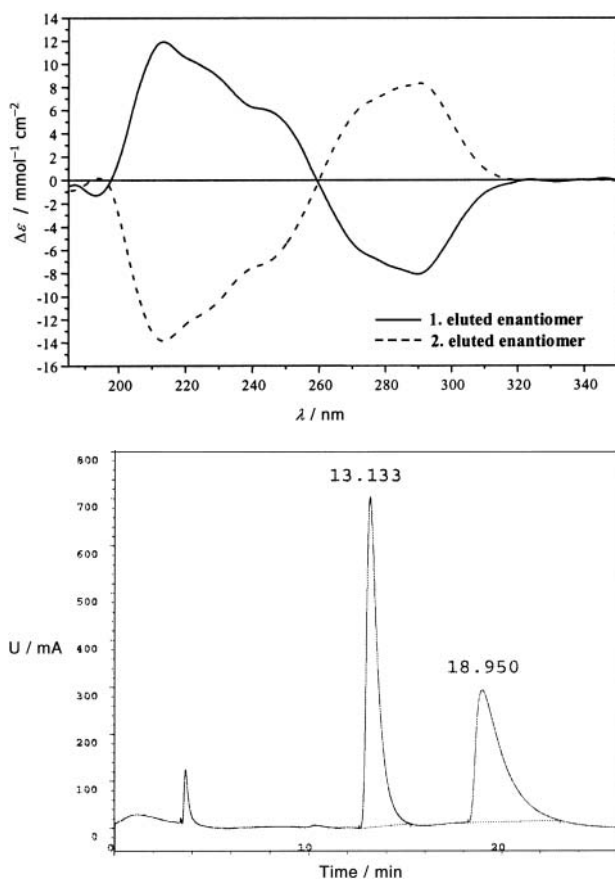


Figure 21. CD spectra of both enantiomers of **TR 44** dissolved in acetonitrile: 1. eluted enantiomer ( $c = 2.393 \times 10^{-4}$  mol dm<sup>-3</sup>,  $l = 0.1$  cm, 100 % ee); 2. eluted enantiomer ( $c = 4.466 \times 10^{-4}$  mol dm<sup>-3</sup>,  $l = 0.1$  cm, 90.6 % ee), accompanied with HPLC for **TR 44** and enantiomers.<sup>59</sup>

resulting **CSP-27–CSP-29** were tested on 14 racemic 4-substituted-dihydropyrimidone derivatives listed in Figure 20, and the results are presented in Table XII.<sup>59</sup>

The results given in Table XII reveal a specific interaction in the enantio-recognition process. Surprisingly, there is no relation between the type of substituent on the C(4) atom in the DHPM ring and separation efficacy. Thus, 4-Me derivative **TR 38** was separated with the same efficacy on all three CSPs ( $\alpha$  1.2–1.3) as most of the 4-aryl substituted analytes ( $\alpha$  1.1–1.4). We have taken this result as an indication of the limited contribution of the 4-aryl group to enantio-recognition, prompted by the previously established *pseudoaxial* position of this group in DHPM derivatives in solution<sup>60</sup> and in the crystal,<sup>61</sup> and confirmed by extensive calculations.<sup>62</sup> An obvious conclusion is that the most probable interactions in the complexes between 4-aryl-DHPM and **CSP-27–CSP-29** are the multiple hydrogen bonding between the analyte and dipeptide-like unit in the CSP, and the  $\pi$ - $\pi$  interaction between DHPM and DNB aromatic units. This interaction places the aryl group at C(4) away from the interacting surface, and orients it towards the DMA unit on the CSP.

Such consideration, however, turned out to be wrong! The results of enantioseparation of **TR 44**, and molecular modeling of the interaction of its enantiomers, and the model of the chiral selector in **CSP-27** revealed a completely different topology of the complex.<sup>59</sup>

The elution order for **TR 44** was determined by running the CD spectra of the separated faster and more retained enantiomers, Figure 21. The more retained enantiomer exhibited a positive CD band at ca 290 nm and a

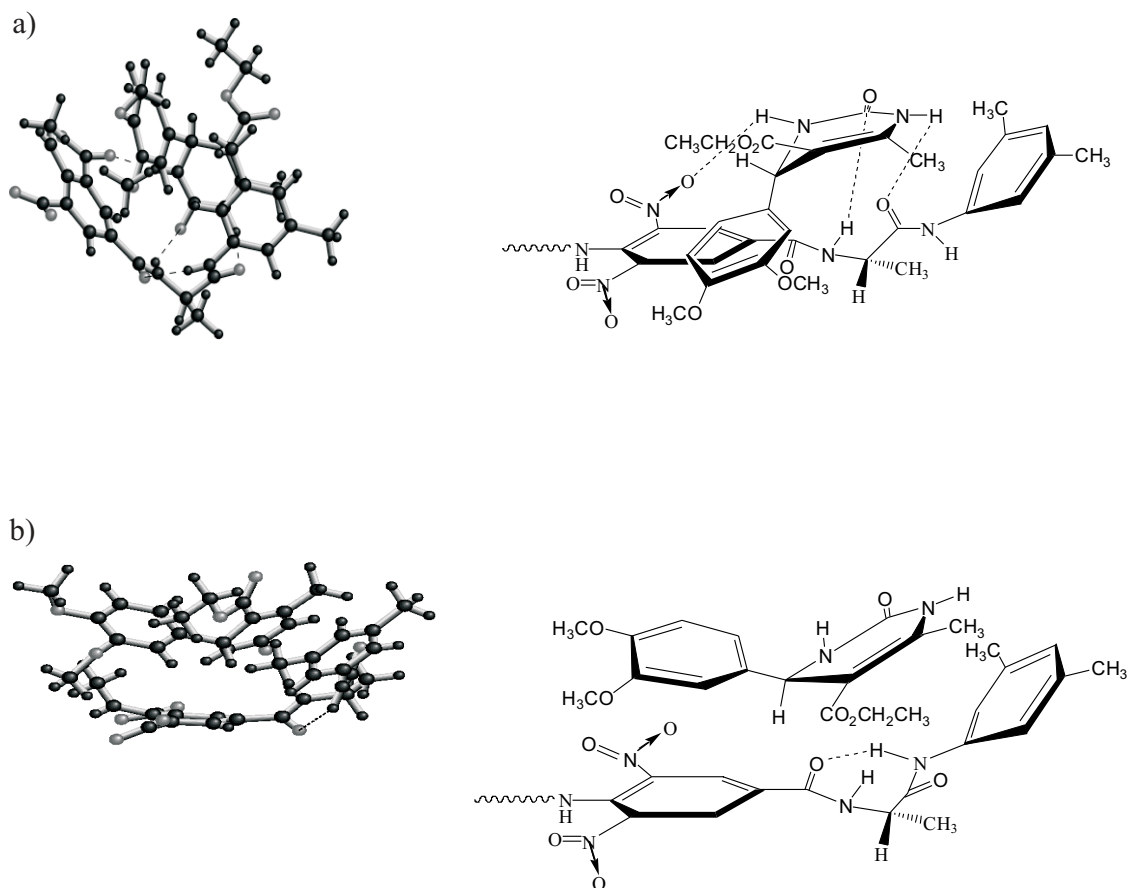


Figure 22. Structures of complexes with the lowest energy, obtained by computational docking of enantiomers of **TR 44** onto **CSP-27**; a) complex with (*S*)-**TR 44**; b) complex with (*R*)-**TR 44**.<sup>59</sup>

negative one at *ca* 210 nm, revealing (*S*)-absolute configuration at C(4), according to the analysis of the CD spectra of 4-substituted DHPM derivatives and the correlation of configuration.<sup>63</sup>

A detailed conformational search for the model selector of **CSP-27** and for both **TR 44** enantiomers was performed. Each of the conformations of **TR 44** enantiomers was then docked onto each conformation of the model of **CSP-27**, followed by molecular mechanics minimization of the resulting complex, which resulted in *ca* 30 000 structures. Figure 22 depicts the lowest energy structure of the complexes found by docking (*S*)- and (*R*)-enantiomers of **TR 44** onto the model of **CSP-27**. The relative stability of these complexes is nicely corroborated by the experimentally determined elution order of enantiomers.

A notable feature of the more stable complex with the (*S*)-enantiomer of **TR 44** is the presence of four hydrogen bonds, which are, for clarity, repeated in the formula beside the computed structure. Additional stabilization comes from the  $\pi$  edge-to-face interaction between the  $\pi$ -electron rich DMA-moiety of **CSP-27** and the  $\pi$ -deficient DHPM unit in the analyte, and the offset stacking between the  $\pi$ -rich dimethoxyaryl unit in the

analyte and the  $\pi$ -electron deficient DNB-group of **CSP-27**. There is a clearly visible chiral cleft, formed by the  $\pi$ -donor and  $\pi$ -acceptor units in **CSP-27**.

## CONCLUSIONS

In conclusion, we expect that the examples presented in this authors' review have shown how a combined experiment and modeling do not only give an insight into the enantioselection process but also have a heuristic value, *i.e.*, the results of such approach can be used with a high level of confidence in designing novel, more effective CSPs. This in particular applies to the group of compounds discussed in the last section. We are actually designing more effective CSPs for separation of other classes of racemic compounds.

*Acknowledgements.* – Figures, tables and shemes have been partly reproduced from the cited references with permission obtained from the American Chemical Society (Ref. 54), Marcel Dekker, Inc. (Ref. 56), Royal Society of Chemistry (Ref. 2), Taylor & Francis (Ref. 40), and Wiley-Liss (Refs. 35, 41, 44, 47, 59). This work was supported by the Ministry of Science and Technology of the Republic of Croatia (Project No 980601), and in part by POLYtech S.c.r.l. (Area Science Park, Trieste, IT).

## REFERENCES

- W. Lindner, *Strategies in Liquid Chromatography Resolution of Enantiomers*, in: R. Janoschek (Ed.), *Chirality – From Weak Bosons to  $\alpha$ -Helix*, Springer-Verlag, 1991, pp. 180–203.
- S. Allenmark and V. Schurig, *J. Mater. Chem.* **7** (1997) 1955–1963.
- I. W. Wainer, *Trends Analyt. Chem.* **6** (1987) 125–143.
- (a) D. Kontrec, V. Vinković, and V. Šunjić, *Kem. Ind.* **46** (1997) 273–285; (b) *ibid.* 345–349.
- G. Subramanian (Ed.), *Chiral Separation Techniques*, Wiley-VCH, Weinheim-Chichester, 2001.
- C. J. Welch, *J. Chromatogr. A* **666** (1994) 3–26.
- W. H. Pirkle and Y. Liu, *J. Chromatogr. A* **749** (1996) 19–24.
- S. Allenmark, *Chromatographic Enantioseparation: Methods and Applications*, Ellis Horwood, New York, 2<sup>nd</sup> Ed., 1991.
- C. A. White and G. Subramanian, in: G. Subramanian (Ed.), *A Practical Approach to Chiral Separation Chromatography*, VCH, Weinheim, 1994, pp. 1–17.
- N. M. Maier, S. Schefzick, G. M. Lombardo, M. Feliz, K. Rissanen, W. Lindner, and K. B. Lipkowitz, *J. Am. Chem. Soc.* **124** (2002) 8611–8629.
- W. H. Pirkle, D. W. House, and J. M. Finn, *J. Chromatogr.* **192** (1980) 143–158.
- C. Wolf and W. H. Pirkle, *J. Chromatogr. A* **799** (1998) 177–184.
- W. H. Pirkle and C. J. Welch, *J. Chromatogr. A* **731** (1996) 322–326.
- M. H. Hyun, S. C. Han, B. H. Lipshutz, J. Y. Shin, and C. J. Welch, *J. Chromatogr. A* **910** (2001) 359–365.
- F. Gasparrini, D. Missiti, M. Pierini, and C. Villani, *J. Chromatogr. A* **724** (1996) 79–90.
- F. Gasparrini, I. D'Acquarica, D. Missiti, M. Pierini, and C. Villani, *Pure Appl. Chem.* **75** (2003) 407–412.
- N. M. Maier and G. Uray, *J. Chromatogr. A* **732** (1996) 215–230.
- G. Uray, W. Stampfer, and W. M. F. Fabian, *J. Chromatogr. A* **992** (2003) 151–157.
- P. Franco, P. M. Klaus, C. Minguillon, and W. Lindner, *Chirality* **13** (2001) 177–186.
- P. Franco, J. Blanc, W. R. Oberleitner, N. M. Maier, W. Lindner, and C. Minguillon, *Anal. Chem.* **74** (2002) 4175–4183.
- S. Allenmark and U. Skogsberg, *Enantiomer* **5** (2000) 451–455.
- L. Thunberg and S. Allenmark, *Chirality* **15** (2003) 400–408.
- A. Iuliano, E. Pieroni, and P. Salvadori, *J. Chromatogr. A* **786** (1997) 355–360.
- A. Iuliano, C. Lecci, and P. Salvadori, *Tetrahedron: Asymmetry* **14** (2003) 1345–1353.
- L. Oliveros, C. Minguillon, B. Desmazieres, and P. L. Desbene, *J. Chromatogr.* **569** (1992) 53–59.
- L. Oliveros, C. Minguillon, and T. Gonzales, *J. Chromatogr. A* **672** (1994) 59–65.
- N. Oi, H. Kitahara, F. Aoki, and N. Kisu, *J. Chromatogr. A* **689** (1995) 195–201.
- N. Oi, H. Kitahara, Y. Matsushita, and N. Kisu, *J. Chromatogr. A* **722** (1996) 229–232.
- M. H. Hyun, Y. J. Cho, J.-J. Ryoo, K. K. Jyung, and G. S. Heo, *J. Chromatogr. A* **696** (1995) 173–183.
- M. H. Hyun, J.-J. Ryoo, Y. J. Cho, and J. S. Jin, *J. Chromatogr. A* **692** (1995) 91–96.
- M. H. Hyun, Y. J. Cho, J. A. Kim, and J. S. Jin, *J. Chromatogr. A* **984** (2003) 163–171.
- Z. Hameršak, M. Hollosi, D. Kontrec, B. Ladešić, Zs. Majer, and V. Šunjić, *Tetrahedron* **51** (1995) 2331–2338.
- D. Kontrec, V. Vinković, A. Lesac, V. Šunjić, and M. Hollosi, *Tetrahedron: Asymmetry* **10** (1999) 1935–1945.
- I. Novak, B. Kovač, D. Kontrec, and V. Šunjić, *J. Electron. Spectr.* **199** (2000) 281–286.
- D. Kontrec, V. Vinković, and V. Šunjić, *Chirality* **11** (1999) 722–730.
- W. Pirkle and C. J. Welch, *J. Liq. Chromatogr.* **9** (1986) 243–249.
- M. H. Hyun, Y. D. Kim, and S. C. Han, *J. High Resol. Chromatogr.* **23** (2000) 333–337.
- M. H. Hyun, Y. D. Kim, S. C. Han, and J. B. Lee, *J. High Resol. Chromatogr.* **21** (1998) 464–470.
- D. Kontrec, V. Vinković, and V. Šunjić, *Chirality* **12** (2000) 63–70.
- D. Kontrec, V. Vinković, A. Lesac, V. Šunjić, and A. Aced, *Enantiomer* **5** (2000) 333–344.
- D. Kontrec, A. Abatangelo, V. Vinković, and V. Šunjić, *Chirality* **13** (2001) 294–301.
- W. H. Pirkle, D. W. House, and J. M. Finn, *J. Chromatogr.* **192** (1980) 143–148.
- IRIS Technologies, Chiris Applications Booklet ([www.iris technologies.net](http://www.iris technologies.net)).
- A. Abatangelo, F. Zanetti, L. Navarini, D. Kontrec, V. Vinković, and V. Šunjić, *Chirality* **13** (2001) 984–992.
- V. Schurig, *Chirality* **10** (1998) 140–146.
- O. Trapp, S. Caccamese, C. Schmidt, V. Bohmer, and V. Schurig, *Tetrahedron: Asymmetry* **12** (2001) 1395–1398.
- V. Vinković, D. Kontrec, V. Šunjić, L. Navarini, F. Zanetti, and O. Azzolina, *Chirality* **13** (2001) 581–587.
- B. Buszewski, M. Jezierska, M. Welniak, and D. Berek, *J. High Resol. Chromatogr.* **21** (1998) 267–281.
- O. Azzolina, S. Collina, D. Vercesi, V. Ghislandi, A. Bonabellio, and M. R. Galmozi, *Il Farmaco* **52** (1997) 449–456.
- K. Otsuka, C. J. Smith, J. Grainger, J. R. Barr, D. G. Paterson, N. Tanaka, and S. Terabe, *J. Chromatogr. A* **817** (1998) 75–81.
- J. Balsells and P. J. Welsh, *J. Am. Chem. Soc.* **122** (2000) 1802–1803.
- M. H. Hyun and W. H. Pirkle, *J. Chromatogr.* **393** (1987) 357–365.
- N. Oi, H. Kitahara, F. Aoki, and N. Kisu, *J. Chromatogr. A* **689** (1995) 195–201.
- C. A. Hunter and J. K. M. Sanders, *J. Am. Chem. Soc.* **112** (1990) 5525–5534.
- C. A. Hunter, K. R. Lawson, J. Perkins, and C. J. Urch, *J. Chem. Soc., Perkin 2* (2001) 651–669.
- A. Ranogajec, D. Kontrec, V. Vinković, and V. Šunjić, *J. Liq. Chromatogr. & Rel. Technologies* **26** (2003) 63–83.
- V. Vinković, D. Kontrec, B. Zafirova, and V. Šunjić, *14<sup>th</sup> International Symposium on Chirality*, Hamburg, Germany, 2002, Book of Abstracts, p. 145.
- C. O. Kappe, *Eur. J. Med. Chem.* **35** (2000) 1043–1052.
- D. Kontrec, V. Vinković, V. Šunjić, O. Kappe, B. Schuik, and W. M. F. Fabian, *Chirality* **15** (2003) 550–557.
- O. P. Kleidering and C. O. Kappe, *Tetrahedron: Asymmetry* **8** (1997) 2057–2067.
- C. O. Kappe, *First Int. Electronic Confer. On Synth. Org. Chem.* (ECSOC-1), Sept. 1–30, 1997.
- W. Krenn, P. Verdino, G. Uray, K. Faber, and C. O. Kappe, *Chirality* **11** (1999) 659–662.
- G. Uray, P. Verdino, F. Belaj, C. O. Kappe, and W. M. F. Fabian, *J. Org. Chem.* **66** (2001) 6685–6694.

## SAŽETAK

### **Ekperiment i model u enantioprepoznavanju pomoću kiralnih stacionarnih faza Pirklovog tipa koje sadrže aromatičku $\pi$ -kiselinsku razgrananu jedinicu**

**Darko Kontrec, Vladimir Vinković, Maja Šepelj i Vitomir Šunjić**

Ukratko su prikazani projekti u laboratoriju autora usmjereni na razvoj novih kiralnih stacionarnih faza (*chiral stationary phase*, CSP). Naglasak je dan na primjenu 2,4,5,6-tetrakloro-1,3-dicijanobenzena i 4-kloro-3,5-dinitrobenzojeve kiseline kao mjesta grananja u Pirklovim (četkolikim) kiralnim stacionarnim fazama. Opisana je priprava skoro stotinu novih CSP-a, koja je zahtijevala sintezu skoro tri stotine novih spojeva kao intermedijara ili modelnih struktura. Posebna svojstva prepoznavanja i djelotvornosti u enantioselekciji pojedinih CSP-a pokazana je na različitim skupinama racemata, koji služe za provjeravanje (*test-racemate*, TR). Raspravljana je odnos između strukture i konformacijskih svojstava kiralnih selektora i racemičnih analita. Razmatrana su posebna svojstva nekih CSP-a, povećanje njihova kapaciteta uvođenjem TWEEZER-ske jedinice u kiralni selektor, kao što je kataliza procesa enantiomerizacije na koloni konfiguracioni nestabilnih analita. Predložen je mehanizam enantioprepoznavanja nekih TR-a sa strukturno sličnim kiralnim stacionarnim fazama.